50777-101

PB91168112

REPORT DOCUMENTATION PAGE	1. REPORT NO.	2.

4. Title and Subtitle LIXIVANT SELECTION FOR MANGANESE IN SITU LEACH MINING - A GEOCHEMICAL APPROACH	5. Report Date 6. TCRC
7. Author(s) Lloyd M. Petrie	8. Performing Organization Rept. No.
9. Performing Organization Name and Address U. S. Bureau of Mines Twin Cities Research Center 5629 Minnehaha Avenue South Minneapolis, MN 55417	10. Project/Task/Work Unit No. 11. Contract(C) or Grant(G) No. (C) (G)
12. Sponsoring Organization Name and Address U. S. Bureau of Mines Research 2401 E. Street, NW Washington, DC 20240	13. Type of Report & Period Covered 14. Open File Report
15. Supplementary Notes	

16. Abstract (Limit 200 words) The Bureau of Mines is conducting research to identify highly selective chemical lixiviants for in situ leach mining of critical and strategic minerals from domestic low-grade ores. This report presents part of that effort by 1) reviewing chemical lixiviants for manganese, 2) describing mineral dissolution models, and 3) presenting a geochemical approach to lixiviant selection and optimization called geochemical characterization. Geochemical characterization logically follows geologic characterization (i.e. ore petrology) by focusing on leaching chemistry at mineral surfaces. It consists of interrelated 1) theoretical modeling and 2) lab experimentation which lead to lixiviant systems specifically suited for a given ore body. This report focuses on the theoretical modeling necessary to develop selective lixiviants. This modeling consists of 1) thermodynamic and 2) kinetic evaluations of prospective lixiviant-ore combinations that favor commodity metal leaching over gangue leaching. Kinetic evaluation uses a number predictive methods for leaching reactivity, including inorganic solution chemistry and molecular orbital theory. This thermodynamic and kinetic evaluation process is illustrated in a study of selective SO_2 leaching of domestic manganese minerals. Geochemical reaction mechanistic reasons exist for observed leaching rate differences among manganese oxide minerals. Rapid SO_2 leaching of manganese oxides is thermodynamically and kinetically favored. Molecular orbital theory reveals that SO_2 has an ideal structure to directly bond and reduce Mn^{4+} to water-soluble Mn^{2+} more rapidly than Mn^{3+}.

17. Document Analysis a. Descriptors

b. Identifiers/Open-Ended Terms

c. COSATI Field/Group

REPRODUCED BY
U.S. DEPARTMENT OF COMMERCE
NATIONAL TECHNICAL
INFORMATION SERVICE
SPRINGFIELD, VA 22161

18. Availability Statement	19. Security Class (This Report)	21. No. of Pages
	20. Security Class (This Page)	22. Price

FINAL

3/4

CONTENTS

Preceding page blank

Preceding page blank

ILLUSTRATIONS

TABLES

LIXIVIANT SELECTION FOR MANGANESE IN SITU LEACH MINING: A GEOCHEMICAL APPROACH

By Lloyd Petrie[1]

*** ABSTRACT

The Bureau of Mines is conducting research to identify highly selective chemical lixiviants for in situ leach mining of critical and strategic minerals from domestic low-grade ores. This report presents part of that effort by (1) reviewing chemical lixiviants for manganese, (2) describing mineral dissolution models, and (3) presenting a geochemical approach to lixiviant selection and optimization called geochemical characterization. Geochemical characterization logically follows geologic characterization (i.e. ore petrology) by focusing on leaching chemistry at mineral surfaces. It consists of interrelated (1) theoretical modeling and (2) lab experimentation which lead to lixiviant systems specifically suited for a given ore body.

This report focuses on the theoretical modeling necessary to develop selective lixiviants. This modeling consists of (1) thermodynamic and (2) kinetic evaluations of prospective lixiviant-ore combinations that favor commodity metal leaching over gangue leaching. Kinetic evaluation uses a number predictive methods for leaching reactivity, including inorganic solution chemistry and molecular orbital theory.

[1] Research Chemist
Twin Cities Research Center, Bureau of Mines, Minneapolis, MN.

This thermodynamic and kinetic evaluation process is illustrated in a study of selective SO_2 leaching of domestic manganese minerals. Geochemical reaction mechanistic reasons exist for observed leaching rate differences among manganese oxide minerals. Rapid SO_2 leaching of manganese oxides is thermodynamically and kinetically favored. Molecular orbital theory reveals that SO_2 has an ideal structure to directly bond and reduce Mn^{4+} to water-soluble Mn^{2+} more rapidly than Mn^{3+}.

*** INTRODUCTION

The challenges facing the U.S. minerals industry are many in the rapidly changing global economy (1-3); including finding adequate domestic supplies of critical and strategic minerals, facing intense foreign competition, addressing health and safety concerns, preserving natural resources, and reducing pollution. One serious consequence of current market conditions is U.S. dependence on imported supplies of critical and strategic and platinum group minerals that are so vital to our steel, aerospace, electronic, and defense-oriented industries. For example, in 1989 the U.S. imported the following range of percentages of critical commodities (1, p. 25):

- manganese 100 %
- cobalt 86 %
- chromium 79 %
- nickel 65 %
- platinum group 94 %

The United States does have deposits of critical and strategic minerals that could be tapped to reduce the reliance on foreign sources of mineral supply. However, many of these deposits are low grade and cannot be mined conventionally for several reasons. First, many of these deposits lie in wilderness areas where conventional mining would not be allowed. Second, the cost of haulage from the mining area to the mill, including the costs of maintenance, fuel, tires, and drivers, are prohibitive because of the low grade of these deposits. Third, comminution of these ores in the mill, which is needed as a first step in beneficiation processes, is not economical. Fundamental research is therefore needed to develop innovative mining techniques that can reduce or eliminate haulage and comminution costs and is compatible with the environment.

In situ leach mining offers the promise of extracting specific metals from low grade ore at lower capital and operational costs as well as necessary environmental restoration costs. In situ uranium operations have been profitable in Texas while in situ mining of copper with sulfuric acid is being field tested in Arizona (4).

The key to successful implementation of in situ leach mining to critical/strategic and precious metal ore deposits is the development of highly selective in situ leaching systems based on lixiviants that rapidly and efficiently extract target minerals while leaving the host rock minerals in place.

The overall objective of this work is to develop lixiviant systems that can be used to selectively remove manganese and other critical/

strategic or platinum group minerals from low-grade U.S. ores and leave associated gangue undisturbed.

The purpose of this report is to (1) review the state of knowledge regarding chemical lixiviant systems for manganese in situ leach mining and (2) present a lixiviant selection and optimization scheme based on geochemical characterization, i.e. interrelated theoretical modeling and lab experimentation of mineral leaching reactions.

*** ACKNOWLEDGEMENTS

The author thanks Dr. John Pahlman, Group Leader of the Geochemical Applications Group, Advanced Mining Division, Twin Cities Research Center for his technical leadership and review of this manuscript. The author especially thanks Dr. George Luther III, College of Marine Studies, U. of Delaware, Lewes, Delaware for his suggestions and manuscript review, especially pertaining to frontier molecular orbital theory.

*** STATE-OF-KNOWLEDGE OF LIXIVIANT SYSTEMS

CHEMICAL SYSTEMS

The first lixiviants for in situ, dump, heap, and stope leaching have been based on strong mineral acids (i.e. sulfuric, nitric, or hydrochloric acids); ammonia/ammonium carbonate; or cyanide (5). Selectivity of these systems was largely based on controlling the concentration of active leaching species (e.g., H^+ for acids) and strong complexation with a class of metals (e.g., CN^- with transition metals) (6).

A number of selective chemical systems have been proposed: dissolved SO_2, ozone, humic acids, lignochemicals, chlorine gas, and synthetic

complexation compounds such as EDTA. An example of a selective chemical leaching system is treatment of mixed metal ores with dissolved SO_2. Khalafalla and Pahlman (7) leached Pacific sea nodules with dissolved SO_2 solutions and found that manganese, nickel, and cobalt were preferentially leached with respect to copper, iron, and aluminum. Greater than 90 % of the manganese, nickel, and cobalt was extracted while only 20, 5, and 5 % of the iron, aluminum, and copper was coextracted when leaching 20 grams of nodules with 200 ml of 5 wt % SO_2.

Pahlman and Khalafalla (8) followed that work with batch and column leaching of 25 domestic Mn ores with 5-6.4 wt % SO_2 and generally extracted greater than 90 % of the total Mn versus less than 20 % of the total Fe (8). They found that there were differences in extraction efficiencies among the Mn minerals found in the ores. For batch leaching, the following order of leaching efficiency was found:

pyrolusite, romanechite > hausmannite, braunite > rhodochrosite > manganite

The manganese silicate mineral, rhodonite, was not leached with dissolved SO_2 solution in batch leaching tests.

MICROBIOLOGICAL SYSTEMS

The desire for more selective mining and metal processing, particularly for low grade or chemically resistant U.S. ore reserves (e.g., sulfides), has led to considerable new effort in microbiological leaching research (9).

Decker (10) has drawn an analogy between human and microorganism accumulation, processing, assembling, using, recycling, and disposing of metals. Since microbes have been dealing with materials for 3.5 billion

years, they have developed a wide range of highly efficient, selective biochemical schemes. He cited lower energy, pollution, acid consumption, and operating costs; greater flexibility; and lower ore concentrations as key advantages for bioleaching operations. This is balanced against slow leaching rates, capital costs for new plants, and relatively low metal concentrations in leach solutions going into processing plants.

Brinckman and Olson (11, 12) recently described the chemical principles involved in bioleaching. Microorganisms interact with metals to change their chemical state for a number of reasons: (1) to derive energy, (2) to detoxify a metal, and (3) to use the metal as a metabolic building block. These biotransformation reactions occur at three types of sites: (1) inside the microbe cell (endocellular), (2) at or near the cell surface (pericellular), and (3) outside the cell (exocellular).

Ehrlich reviewed advances in microbiological leaching of ores (13, 14). The United States minerals industry has successfully used microbes for heap and dump leaching of low grade copper, uranium from some uraniferous ores, and beneficiation of auriferous pyrite/arsenopyrite ores. Ehrlich anticipates more commercial applications using mineral-microbe systems and proposes the use of mixed cultures to enhance recovery of all commodities of commercial value for a given ore.

Related to in situ leach mining, Johnson and coworkers reported 60-90 % copper recoveries for column leaching of three chalcocite ores using H_2SO_4 and T. ferrooxidans versus 2-25 % with only sulfuric acid (15).

*** BACKGROUND

OVERVIEW OF MINERAL DISSOLUTION PROCESSES

Drever (16) presents an overview of mineral dissolution processes important to lixiviant optimization. Figure 1, adapted from Drever (16), depicts the processes governing the rate of mineral dissolution:

1. Bulk solution transport of the lixiviant toward and reaction products away from the mineral
2. Surface product layer transport of the lixiviant toward and reaction products away from the mineral
3. Chemical reactions at the mineral surface

Underground flow of both native groundwater and lixiviants pumped into an ore body is laminar. Therefore, near solution-mineral interfaces, transport of solution molecules to and from the mineral surface is controlled by a Fick's diffusion mechanism. As some parts of a heterogeneous ore surface are dissolved, the remaining ore matrix will become a porous nonreactive (or slowly reactive) layer called a surface product layer. For example, in the dissolution of the copper silicate mineral, chrysocolla, with H_2SO_4, an unreacted silicate lattice remains as copper is leached from the mineral (17). It follows that diffusion through a surface product layer like the silicate lattice in partially leached chrysocolla would be different than diffusion through the bulk solution.

Actual contact between solution species and the unreacted mineral surface can result in a number of types of chemical reactions (table 1) including physical adsorption, chemisorption or surface complexation, dissolution, precipitation, oxidation-reduction, and biochemical

processes. It should be noted that at any given time there could be a number of different and competing surface chemical reactions occurring. For example, the overall reaction sequence for manganese mineral dissolution involves adsorption, chemisorption, and oxidation-reduction reactions.

Geochemical heterogeneous reactions, including mineral dissolution, can generally be classified as either (1) transport (diffusion) rate-limited or (2) surface chemical reaction rate-limited. In some cases, however, the transport rates are nearly equal to the surface reaction rates. In these cases, both transport and surface reactions control the rate of dissolution.

The solution transport processes and chemical reactions at the mineral surface demonstrate the interrelation between geocharacterization and geochemical characterization during selection and optimization of prospective lixiviant-ore systems. Geologic characterization involves geologic compositional and structural assessment of the ore body to estimate rates of lixiviant contact with target minerals (i.e. transport processes). Geochemical characterization involves assessment of the mechanisms and rates of surface chemical reactions of both target and gangue minerals (i.e. chemical reaction processes). Both geologic characterization and geochemical characterization therefore are needed to fully optimize the prospective lixiviant-ore system for in situ leach mining.

In this report, the mechanisms and rates of key manganese and gangue mineral dissolution reactions will be investigated.

COMPOSITION AND STRUCTURE OF KEY MANGANESE MINERALS

In order to determine the chemical reaction kinetics of manganese ore dissolution reactions, it is necessary to know the composition and structure of key manganese minerals. As with previous applications of in situ leach mining technology, the composition and the structure of the target mineral (i.e. manganese) and the associated gangue will have to be determined for the specific ore body being evaluated for mining. A comprehensive discussion of worldwide manganese deposits, including U.S. deposits, is presented by Roy (19).

Potter and coworkers (18) reported six U.S. locations with significant low grade manganese ore deposits. These are listed in table 2. Pahlman and Khalafalla (8) reported on SO_2 leaching of manganese ores, including a number of samples from the above six deposits. Table 3 is a reproduction of table 1 from Pahlman and Khalafalla's report. In addition to manganese mineralogy, table 3 lists the principal gangue mineralogy. Gangue minerals competition with commodity minerals is an important consideration during in situ leach mining optimization. Oxides are the most common and abundant mineralogy for the U.S. manganese ore deposits, followed by carbonates and silicates. Table 4 summarizes the composition and structure for the key manganese minerals found in U.S. manganese ore deposits, including the valence and coordination number of manganese metal centers.

It has been estimated that approximately 46% of the total U.S. manganese ore reserves are located in the Cuyuna North Range of east-central Minnesota. Four manganese minerals have been found to be predominant in this large low grade manganese ore deposit, and the

compositional formulae; the crystal structure, oxidation state of manganese centers, and the coordination number of the manganese centers of these manganese minerals have been listed in table 5. Pyrolusite and manganite are the most abundant manganese oxides on the Cuyuna Range, while rhodochrosite is also quite common. Chief gangue minerals include an Fe^{3+} silicate called acmite or aegirine, which has the compositional formula $NaFeSi_2O_6$, chert, and hematite.

From a geochemical kinetics perspective, there are several observations to be made from the data in table 4. First, these minerals have manganese centers with a range of oxidation states (4+, 3+, 2+). The charge on a manganese center significantly affects the chemical stability and dissolution reactivity of the mineral. Second, manganese centers usually have a bonding coordination number of six, indicating the octahedral bonding symmetry common to manganese ions in solution. Third, oxygen is the most common element bonded to manganese. Fourth, the structural differences of manganese minerals do vary enough to possibly affect dissolution reactivity. For example, the basic unit for pyrolusite, $[Mn^{4+}O_6]$, and for manganite, $[Mn^{3+}(O,OH)_6]$, form relatively tight chain structures, whereas romanechite consists of triple chains of $[Mn^{4+}O_6]$ units that form open tunnels (20). This means that more romanechite Mn sites may be available for dissolution by lixiviant than pyrolusite or manganite manganese sites.

PREVIOUS RESEARCH ON MANGANESE ORE DISSOLUTION

Much research has been reported on the dissolution of manganese ores and single manganese minerals. The work reviewed is only that which pertains directly to mining or minerals processing.

Selective Oxide Dissolution with Dissolved SO_2

One lixiviant, sulfur dioxide (SO_2), has been extensively investigated since it is capable of rapidly dissolving acid resistant manganese oxides such as pyrolusite. SO_2 bubbled into water forms an acidic solution originally called "sulfurous acid". In fact, earlier work centered on the preparation of sulfur oxide acids using MnO_2 suspensions. The first published report was the preparation of dithionic acid ($H_2S_2O_6$) by Gay-Lussac and Welter (21). The first detailed investigation of SO_2 and manganese oxide chemistry was reported by Meyer and Schramm (22), who found that manganous sulfate ($MnSO_4$) and manganous dithionate (MnS_2O_6) were formed.

The Bureau has a long involvement in the processing of low-grade manganese ores with SO_2 solutions. The early Bureau work was reviewed in a Bureau Information Circular by Dean, Leaver, and Joseph (23), which detailed hydrometallurgical processes using SO_2.

Wyman and Ravitz (24) discussed the selective nature of SO_2 leaching for manganese over iron and other gangue in domestic ores. They determined the composition of the final leachates and did not construct detailed composition vs. time (or SO_2 amount) leaching curves.

Important progress in understanding the chemistry of SO_2 and manganese oxides was reported by Bassett and Parker (25), who conducted anaerobic batch leaching experiments with SO_2 and a variety of manganese salts. By measuring reaction products at the end of the experiment, they theorized that two separate mechanisms were responsible for formation of $SO_4^=$ and $S_2O_6^=$. $MnSO_4$ was formed by oxide surface reactions involving a single 2-electron transfer to form $SO_4^=$ at the mineral

surface. The $S_2O_6^=$ was formed by two separate 1-electron transfer reactions, which could include an intermediate Mn^{3+} complex. Since the percentages of $S_2O_6^=$ and $SO_4^=$ varied with the structure of the manganese oxide mineral, they deduced that the oxidation of sulfurous acid must be occurring at the mineral surface and not in solution. They did not have the experimental means to confirm their conclusions.

Later work by Higginson and Marshall (26) supported Bassett and Parker. Using a number of different oxidants in solution, they found 1-electron transfer oxidants (e.g. Fe^{3+}, Co^{3+}) produced $S_2O_6^=$ while 2-electron transfer oxidants (e.g. IO_3^-, H_2O_2) produced $SO_4^=$. Their explanation for these results was that 1-electron transfer produces an intermediate free radical, $*SO_3^-$, which dimerizes to form $S_2O_6^=$.

Back, Ravitz, and Tame (27) reported SO_2 processing of MnO_2 ores under aerobic conditions. They observed decreased $S_2O_5^=$ formation with lowered pH and increased agitation (i.e. increased solution oxygenation). For example, only 3 % $S_2O_6^=$ was formed at pH 0.75 vs. 8 % at pH 1.90 for well agitated systems. This work was part of the research for the "dithionate process" that was developed by the Bureau for processing low-grade manganese dioxide ores.

Herring and Ravitz (28) reported the first actual reaction rate data for anaerobic SO_2 - manganese dioxide reactions. By then the chemical behavior of SO_2 gas bubbled into water was better characterized. Specifically, SO_2 gas molecules are not strongly hydrolyzed and remain as separate molecular species at low pH. As the pH is raised, bisulfite (HSO_3^-) is first formed and then sulfite ($SO_3^=$) begins to form:

$$SO_2 + H_2O = H^+ + HSO_3^- = SO_3^= + 2H^+$$

For example, at pH 1.0 approximately 85 % of SO_2 bubbled into water remains as SO_2 with the rest becoming HSO_3^-. However, at pH 4.0 only 0.5 % remains as SO_2 while 99.5 % becomes HSO_3^-.

Herring and Ravitz found that the rate of manganese dioxide reductive dissolution was faster at lower pH values, for example, 7.6 micromole min^{-1} $(cm^2)^{-1}$ at pH 1.82 vs. 80.4 micromole min^{-1} $(cm^2)^{-1}$ at pH 1.09. These results indicated that manganese dissolution was approximately 10 times faster for SO_2 than for HSO_3^- . The reaction rates were also faster with increasing stirring rate, indicating a transport-controlled reaction. This was confirmed by a low apparent activation energy of 4.5 $\pm$ 0.2 kcal $mole^{-1}$.

A number of researchers have since reported work to further optimize the mineral processing of manganese oxides, particularly pyrolusite, with dissolved SO_2 solutions (29-35). Some of these reports investigated the mechanism and rate of manganese oxide dissolution; i.e., the geochemistry of the process.

Henn, Kirby, and Norman (29) reviewed the 10 major processes for manganese ore which employed SO_2. Nine of the processes used SO_2, H_2SO_4, or a combination of SO_2 and H_2SO_4. The tenth process used a SO_2 roast at 600° to 850° C before a water leach.

Miller and Wan (31) reported work devoted to the kinetics of reductive dissolution of electrolytic MnO_2 and pyrolusite. They concluded that the leaching process was rate-limited by a mineral surface reduction reaction obeying the following rate law:

$$\text{Rate} = d(MnO_2)/dt = k^* K_a^{0.5} A_c [SO_2]_{total}^{0.5} ([H^+]/[H^+] + K_a)^{0.5}$$

where k^* = heterogeneous rate constant

K_a = equilibrium constant for $SO_2 + H_2O = H^+ + HSO_3^-$

A_c = active surface area of MnO_2 mineral

In contrast to Herring and Ravitz (28), Miller and Wan calculated an apparent activation energy of 8.6 kcal $mole^{-1}$ and found no change in rate constants with changes in stirring rate. They cited the latter as evidence that dissolution is controlled by the mineral surface chemical reaction. One explanation for these different conclusions may be found in the difference in experimental conditions used by the two research teams. One significant difference was the geometry of manganese samples. Herring and Ravitz (28) mounted electrolytic MnO_2 in lucite creating a flat plane of reactive mineral sites, whereas Miller and Wan used suspended -25, +48 mesh particles.

In an effort to clarify the mechanism; Asai, Hegi, and Konishi (33) reported an chemical engineering study of an aerobic packed bed of MnO_2 leached with SO_2 and H_2SO_4. Their experimental mass transfer coefficients for SO_2 correctly solved the mass transfer equation for diffusion-controlled transport in a packed bed. Therefore, the surface leaching reaction was not rate-limiting. They reported increased $S_2O_6^=$ formation with increased SO_2 concentration and increased lixiviant flow rate through the column. They also found predominant formation of $MnSO_4$ with large concentrations of SO_2 in the reactor.

Dixit and Raisoni have reported their work in two recent reports. In the first report (34), they demonstrated that sufficiently high concentrations of dissolved O_2 will suppress the reductive dissolution of MnO_2 with SO_2. Viewed from a geochemical perspective, this is a reminder that reductive dissolution of MnO_2 does require an overall

reducing solution environment, i.e. a low Eh value. In their second report (35), dissolution rates of MnO_2 fit the metallurgical equation for diffusion-controlled release of Mn^{2+} through an unreacted product layer:

Dissolution Rate = $kt = 1 - 2/3\ a - (1 - a)^{2/3}$

where k = rate constant

t = time

a = fraction manganese leached

In addition to the research on the use of SO_2 for manganese oxide processing, important work has also been reported on the dissolution of ferromanganese nodules with SO_2. In 1978 Lee and coworkers (36) investigated the effects of water, SO_2, and temperature on the dissolution of Pacific Ocean nodules. The amount of $S_2O_6^{=}$ vs. $SO_4^{=}$ formed during reductive dissolution decreased with increased O_2 concentration and temperature (table 6).

In 1981 Khallafalla and Pahlman (7) reported an important Bureau study that demonstrated the use of SO_2 for selective extraction of critical and strategic metals (i.e. Mn, Co, Ni) from Pacific ferromanganese modules. For a series of batch leaching experiments, they observed that increasing molar ratios of SO_2 in the lixiviant to grams of nodules leached resulted in a reproducible sequence of different metals being preferentially leached:

Mn > Ni > Co >> Fe, Al, Cu

first last

Figure 2, reproduced with permission of the authors, shows their results and demonstrates the dramatic selective preference of SO_2 for

Mn, then Ni and Co. Fe, Al, and Cu were leached only after most of the Mn, Ni, and Co had been leached. Khalafalla and Pahlman used a SO_2 complexation reaction mechanistic theory to explain the selectivity of SO_2 for manganese oxide nodule sites. First, the Mn^{4+} metal centers in the MnO_2 lattices are reduced by SO_2 to Mn^{3+} or Mn^{2+}. Then, other SO_2 molecules act as Lewis acids and exchange with the protons of exposed oxygens that have been protonated:

$$Mn(OH)_2 + 2SO_2 = Mn(O\text{-}SO_2)_2^{2-} + 2H^+$$

They proposed that additional work be conducted to clarify and confirm the proposed mechanisms. If SO_2 complexation of reduced metal centers enhances dissolution of the mineral lattice, then perhaps the speed and selectivity of SO_2 demonstrated above can be related to the relative complexation kinetics of SO_2 with Mn, Ni, Co, and gangue metal centers. In other words, a detailed study of the basic inorganic chemical kinetics of SO_2 complexation with transition metals may provide a logical explanation of the selective leaching properties of dissolved SO_2.

Of the many excellent research reports dealing with the rapid SO_2 dissolution of manganese ores, the 1988 report by Pahlman and Khallafalla (8) may be the most relevant to in situ leach mining. In that report, they presented very encouraging new results from batch and column leaching experiments of 25 U.S. manganese ores exposed to 5 wt % SO_2 solutions. First, they were able to achieve typically greater than 90% Mn recoveries while solubilizing less than 3% of Fe from hematite (Fe_2O_3), a key gangue mineral. Less abundant Fe carbonate (siderite) and hydroxide (goethite) readily dissolved in SO_2 solution. Second, at

low SO_2 application rates (1 mL/min) to the column, calcite ($CaCO_3$) solubilization was minimized by formation of an insoluble $CaSO_3$ outer layer, stopping further leaching of $CaCO_3$. Lastly and very importantly, the slow application of SO_2 lixiviant was still able to leach Mn in ore with low permeabilities (10^{-2} to 10^{-4} darcy). This result strongly supports the argument that rapid leaching of Mn minerals in the ores open more channels for lixiviant penetration further into the ore body, hence geochemically-induced permeability.

In summary, several significant conclusions can be drawn from past research:

1. Aqueous SO_2 is a rapid and efficient lixiviant for manganese minerals, particularly manganese oxides.
2. SO_2 will preferentially select manganese oxides for dissolution before oxides of cobalt, nickel, iron, and other abundant transition metals in ocean nodules and domestic low-grade manganese ore.
3. SO_2 leaching is less rapid for Mn carbonates and silicates.
4. Solution leaching of manganese ores has long been studied, primarily from a mineral processing point of view.
5. The Mn-SO_2 leaching reaction mechanism and rates have been little studied in a geochemical setting. For example, why are Mn^{4+} oxides more easily leached than Mn^{3+} oxides, carbonates, and silicates?

In order to optimize an SO_2 lixiviant system for in situ leach mining applications, it will be necessary to know the intrinsic dissolution kinetics of key manganese and gangue minerals. This can be accomplished by (1) building on the previous research knowledge, (2) applying recent mineral dissolution models, and (3) conducting detailed kinetics experiments under simulated in situ leach mining conditions.

Other Lixiviants for Manganese Ore Dissolution

In addition to the extensive research performed on SO_2 leaching of manganese oxides, a number of other chemical lixiviants, generally strong reductants, have been used to leach manganese minerals. Some of these valuable metallurgical reductants may be adaptable to an in situ leach mining process.

Warren and Devuysst (37) reported hydrazine hydrate ($N_2H_4.H_2O$) extracted 90% of Mn from minus 65, plus 150 mesh pyrolusite in one hour. Hydrazine hydrate is a strong reductant but its high cost at the time prevented its consideration for commercial use.

Malati, Rophael, and Bhayat (38) used $N_2H_4.H_2O$, followed by pyrophosphate ($H_2P_2O_7$), to reduce electrolytic γ-MnO_2 and β-MnO_2. They also reported that the reduction product of the Mn oxides with $N_2H_4 \cdot H_2O$ was $Mn^{3+}OOH$.

Following substantial research on manganese nodule dissolution with mineral acids, Han and Fuerstenau (39) performed leaching experiments on -48 mesh nodule particles using SO_2 and hydroxylamine hydrochloride ($(NH_3OH)Cl$) solutions. For their experimental conditions, $(NH_3OH)Cl$ was more effective (100% vs. 80% Mn^{2+} recovery) and more rapid in reaching

steady state leaching (< 60 min. vs. 90 min.) than SO_2. Once again, the high cost of $(NH_3OH)Cl$ has discouraged its commercial use.

After investigating a number of strong reducing agents, Usatenko and Ryl'kova (40) reported that potassium iodide (KI) was the most effective reductant for pyrolusite and romanechite in manganese ores. Using 20 wt. % KI in 0.3-0.4 M acetic acid, they dissolved 96 to 99 % of the pyrolusite and romanechite present. They also suppressed reduction of manganite by adding EDTA to prevent the further reduction of Mn^{3+} metal centers in manganite to water-soluble Mn^{2+}.

Dresler (41) reported very rapid leaching of γ-MnO_2 with nitrous acid (HNO_2) solutions. Since his stirred reaction cell was similar to Herring and Ravitz's SO_2 leaching cell for γ-MnO_2 (28), Dresler compared overall leaching rates between his HNO_2 work and their SO_2 research. The overall leaching rates for HNO_2 were reported to be "slightly higher than those in sulfurous acid". It should be noted that the NO_2^- has the same electron configuration as SO_2. Therefore, HNO_2 could be a promising potential lixiviant for in situ leach mining if the costs to produce nitrous acid were reasonable and no environmental problems were introduced.

Recently, Dobos (42) reported the effective use of a strong-acid cation exchange resin to accelerate and recover metal carbonates including rhodochrosite ($MnCO_3$) during acid leaching. The resin was added to a sulfuric acid suspension containing 19 wt. % manganese ores. Optimization of the process was performed for such variables as temperature, pH, and supporting electrolyte (i.e. NaCl). Kinetic data were presented.

*** USE OF GEOCHEMICAL CHARACTERIZATION FOR LIXIVIANT SELECTION

Having reviewed (1) the state of knowledge for in situ leach mining lixiviant for manganese, and (2) the mineralogy of key manganese minerals, a question follows: How does one develop a lixiviant for underground use that will selectively dissolve manganese minerals while leaving gangue in place.

An approach to development of selective lixiviants will now be presented that centers on the geology and geochemistry of target ore bodies. It will be called geochemical characterization to emphasize its close relationship to geologic characterization. Geochemical characterization (figure 3) is an interactive lab experimentation and geochemical modeling process that begins with ore petrology, proceeds through basic mineral geochemistry, and concludes with generation of in situ leach mining design parameters.

This report will focus on two theoretical evaluation approaches to lixiviant selection and optimization, one based on thermodynamic considerations and one based on kinetic considerations. Both the thermodynamic and kinetics approaches are molecular views of the geochemical reactions occurring at the lixiviant-mineral interfaces.

To more efficiently conduct the thermodynamic and kinetic evaluations, it is helpful to simplify the mineral dissolution process by initially separating solution transport effects from the mineral surface reactions. Then experiments can be done to verify the theoretical predictions and to measure intrinsic (i.e. without transport effects) geochemical leaching rates.

Furthermore, separation of geochemical reactions from transport effects is reasonable since the selectivity of a lixiviant is more related to its geochemical reactivity with mineral surfaces than its transport properties in an ore body. This assertion is based on the fact that when the lixiviant contacts an ore surface, dissolution selectivity will be based on both (1) the thermodynamic tendency of commodity and gangue leaching reactions to occur and (2) the relative rates of these competing geochemical leaching reactions. It follows that selection and optimization of lixiviants for a given manganese ore body requires an in-depth knowledge of the geochemistry of the key manganese minerals and gangue present.

To illustrate the potential value of geochemical characterization, a thermodynamic and chemical kinetic approach will now be used to evaluate the results for batch leaching of U.S. manganese ores with 6.4 wt % SO_2 at pH 1.1 (Pahlman and Khalafalla (8)). At pH 1.1, approximately 82 mole % of the S is present as SO_2 with the remainder as HSO_3^-. Batch tests were selected for this geochemical characterization because the small size of the ore particles (< 0.841 mm) largely eliminate transport effects. Also, the high SO_2 concentration (6.4 wt %) simplified interpretation since the lixiviant was in large excess compared to the amount of ore particles. Therefore, batch tests represent experimental cases where leaching rates at the mineral-lixiviant interface dictate the extraction efficiency for different manganese ores.

Table 7 summarizes the extraction efficiencies for Mn, Ca, and Fe in batch leaching of manganese ores containing one or two of the seven key

manganese minerals found in U.S. manganese ore reserves (table 4). The following data represent a broad treatment of the data reported by Pahlman and Khalafalla since the averaged values represent efficiency averages from different ore bodies.

The first key observation from the batch leaching data is the wide variation in leaching efficiency among the manganese minerals:

pyrolusite (β-$Mn^{4+}O_2$), romanechite ($Ba(OH)_4Mn^{2+}Mn^{4+}{}_8O_{16}$)	95 %
hausmannite ($Mn^{2+}Mn^{3+}{}_2O_4$), braunite ($Mn^{3+}{}_2O_3)_3Mn^{2+}SiO_3$)	79 %
rhodochrosite ($Mn^{2+}CO_3$)	67 %
manganite (γ-$Mn^{3+}OOH$)	59 %

Rhodonite ($Mn^{2+}SiO_3$) was not measurably leached during the 30-minute experiments. This observation leads to the first question to be answered for lixiviant selectivity and optimization: What is a geochemical explanation for leaching efficiency differences among the manganese minerals?

The second observation is that Ca was significantly leached in many of the samples, regardless of the manganese mineralogy. This observation leads to the second question to be answered for lixiviant selectivity and optimization: What can be done to minimize leaching of Ca during Mn mineral leaching?

The third observation is that Mn was preferentially leached with respect to Fe for all manganese mineral sample types but rhodonite. This observation leads to the third question to be answered for lixiviant selectivity and optimization: What can be done to minimize leaching of Fe during Mn mineral leaching?

THERMODYNAMIC EVALUATION: SO_2 LEACHING OF MANGANESE ORES

Manganese Minerals

Thermodynamic evaluation with respect to manganese minerals is based on the following hypothesis:

> Optimization and selectivity during leaching of manganese ores is based on rapid establishment of thermodynamic equilibria or steady state (for irreversible reactions) for the major leaching reactions.

The thermodynamic approach begins with selection of the most probable chemical reaction that describes dissolution of both manganese and gangue minerals. Then Gibbs standard free energy (ΔG°) is calculated for each reaction (45). The experimental conditions for the work of Pahlman and Khalafalla were close to standard conditions (i.e. 25°C and 1 atm). If the above hypothesis is correct, then those reactions with the most negative free energy will release the most Mn, Ca, or Fe dissolution products into solution.

Table 8 shows such a thermodynamic evaluation for leaching of the seven key Mn minerals in 6.4 wt % SO_2 lixiviant at pH 1.1. The Mn mineral reactions are listed in descending order of experimental leaching efficiency. The probable overall dissolution reactions were selected from the literature and from the knowledge that Mn^{2+} is the only oxidation state of manganese that is both soluble and thermodynamically stable in water. Although Mn^{3+} is soluble, it will slowly disproportionates in acidic water to form Mn^{2+} and insoluble MnO_2 (45):

$$2Mn^{3+} + 2H_2O = 2Mn^{2+} + MnO_2(s) + 4H^+$$

The probable reaction equations also include the oxidation state of Mn metal centers in the minerals. Note that most of the manganese in these minerals exist as +4 and +3 centers bonded to six oxygen atoms.

This leads to the first observation that most manganese mineral leaching reactions must involve reduction of Mn centers to thermodynamically stable Mn^{2+}. This means that of the three S species that comprise the SO_2 equilibrium in water ($SO_2 + H_2O = H^+ + HSO_3^- = 2H^+ + SO_3^=$), SO_2 is the most important since it is a reductant. Both HSO_3^- and $SO_3^=$ are oxidants.

The second observation regarding table 8 is that most of the manganese minerals leaching reactions have negative ΔG° values and are favored to occur in SO_2 solutions at experimental conditions. Interestingly, even though the leaching reaction for rhodochrosite with H^+ ions was the least favored thermodynamically ($\Delta G^\circ = 0$), Mn^{2+} was readily released into the pH 1 SO_2 lixiviant.

The third observation relates to the previous optimization question concerning the difference in Mn extraction efficiencies among the seven manganese minerals. The thermodynamic data in table 8 are listed by mineral in their descending extraction efficiency as found by Pahlman and Khalafalla (8). If the batch leaching reactions were all at equilibria, then the ΔG° values should be less negative in reading down the table. Such a correlation is only partially demonstrated. The -209 kJ/mole ΔG° for pyrolusite and romanechite reductive dissolution to form $SO_4^=$ and Mn^{2+} is the most negative value. However, differences in Mn extraction efficiencies among the other five manganese minerals cannot be clearly explained by this thermodynamic evaluation. The ΔG° values

for hausmannite (-110 kJ/mole), braunite Mn_2O_3 sites (-131 kJ/mole), and manganite (-132 kJ/mole) are all approximately the same. Thermodynamically, rhodochrosite is the least favored manganese mineral for leaching but Mn was readily extracted from it (67% average). Likewise, the rhodonite leaching reaction had a negative ΔG° (-67 kJ/mole) but was not leached in measurable amounts during the 30 minute experiments.

Two possible explanations are offered for these observations. First, the important hypothesis that thermodynamic equilibria or steady state is attained may not be valid for these experiments as some or all of the manganese leaching reactions were too slow to reach equilibrium and attain maximum leaching rates. This would explain why manganite, with a more negative ΔG° than hausmannite, would not leach as rapidly during the batch leaching experiments. The intrinsic rate of manganite leaching was simply much slower than the rate for hausmannite.

Second, some of the probable overall leaching reactions proposed in table 8 may not be those which are actually occurring, despite their reasonableness for these experimental conditions. This is certainly possible and highlights the limitations of the knowledge about leaching kinetics for many of the major manganese minerals. As discussed in the BACKGROUND section, most previous SO_2 leaching research has been restricted to pyrolusite and other forms of MnO_2 (22, 24, 25, 28, 31, 33, 35). The basic kinetics information, including overall leaching reactions, is simply not yet available for all the key manganese minerals in U.S. ores.

Based on the comparisons between leaching efficiencies (table 7) and the thermodynamic evaluation of probable leaching reactions (table 8), several conclusions can be reached:

1. Most manganese minerals are thermodynamically favored for leaching in high SO_2, low pH lixiviants.
2. Since only Mn^{2+} is stable and soluble in water, manganese oxides must undergo a reduction reaction as part of leaching. SO_2 has been shown to be a very effective reductant for this purpose.
3. In this 30 minute batch leaching experiment, some of the manganese leaching reactions were too slow to reach equilibrium.
4. More basic research is needed to determine overall reaction formulae for most of the seven key manganese minerals.

Therefore, it is concluded, that both thermodynamic and kinetic (leaching speed) factors govern the relative differences in leaching efficiencies among the seven manganese minerals.

Gangue Minerals

Thermodynamic evaluation can also be used to assess the relative tendency of key gangue minerals to be leached by 6.4 wt % SO_2 at pH 1. This evaluation is found in table 9. Not surprisingly, quartz is not favored to leach. According to free energies for overall reaction equations, calcite is only slightly favored for leaching in acidic lixiviants as are hematite and geothite. Siderite was not thermodynamically favored for leaching.

One surprising observation from table 9 is that none of the gangue leaching reactions are strongly favored according to thermodynamics. The ΔG° values for two of the three favored reactions (-36, -5, and -2 kJ/mole) are an order of magnitude less negative than ΔG° values for the

manganese minerals. This certainly supports the experimental observation that Mn leaching was more efficient than Fe leaching. Despite the higher thermodynamic tendency for leaching manganese oxides compared to calcite, a majority of total Ca was released during the experiments. This indicates that calcite leaching is fast.

Since release of both Fe^{3+} and Ca^{2+} results from H^+ - driven leaching reactions, one obvious way to minimize these unwanted gangue reactions is to operate at the highest possible pH that will permit satisfactory SO_2 leaching of the manganese minerals. When only manganese oxides are present, it may be possible to operate at pH 2-3 to suppress calcite and Fe mineral leaching but still have SO_2 reductive dissolution for Mn^{2+}.

In summary, this simple thermodynamic evaluation of SO_2 leaching of U.S. manganese ores has been a useful beginning to lixiviant optimization. Since most manganese minerals require reduction of metal centers to Mn^{2+}, SO_2 is the S species of interest. Most key manganese minerals found in the significant U.S. deposits of manganese are thermodynamically favored for leaching. However, the incomplete correlation between Gibbs standard free energies and the leaching efficiencies of the seven key manganese minerals (table 7 and 8) strongly suggests that leaching was not a complete thermodynamic equilibrium. This suggests that a study of SO_2 - manganese mineral geochemical kinetics would further assist lixiviant optimization.

KINETIC EVALUATION: SO_2 LEACHING OF MANGANESE ORES

Overview of Chemical Kinetics

Chemical kinetics is the study of the rate and stepwise sequence of reaction steps for a given chemical reaction represented by its

stoichiometric overall equation. This stepwise sequence of elementary reactions is called the mechanism of the reaction.

Kinetic evaluation of SO_2 leaching of manganese ores uses a different hypothesis than thermodynamic evaluation:

> Optimization and selectivity during leaching of manganese ores is based on the relative rates of competing leaching reactions of the individual manganese and gangue minerals.

It was reasonable to begin lixiviant optimization by hypothesizing that a given lixiviant-ore leaching process rapidly reaches equilibrium or steady state. This is the simplest geochemical leaching process to evaluate and some natural geochemical systems do reach equilibria or steady state if the residence times are long enough (46). In fact, one can view equilibrium or steady state as a limiting case of geochemical leaching kinetics where the important reactions are rapid enough to result in constant solution concentrations of reaction products.

During the last three decades substantial progress has been made in understanding geochemical and natural waters thermodynamics. For water systems, reasonably accurate equilibrium models have been created for predicting the chemical forms (i.e. speciation) of elements given pH, Eh, ionic strength, and total concentrations of cations and anions (47).

In this decade, evidence has appeared suggesting that many geochemical processes, including mineral dissolution, may not always be at equilibria or steady-state (46, 48, 49, 50, 51). Correspondingly, research efforts are accelerating in the field of geochemical kinetics. The interest in geochemical kinetics was underscored at a recent workshop on metal speciation and transport in groundwater by the following appeal made by James J. Morgan (48):

"In brief, the ground of speciation research and applications is necessarily shifting from $dC_i/dt = 0$ as paradigm, to $dC_i/dt = R_{ij}$ for all processes affecting the concentrations of metals (and neighboring non-metals of the periodic table) in aquatic systems. The notion of speciation itself must be seen as extending to solids and surfaces, as well as aqueous solutions."

Kinetic evaluation of a geochemical reaction, such as mineral leaching, requires a more intimate knowledge of the reaction and much more experimental data than that required for a thermodynamic evaluation (51, 52). Kinetic information is summarized in the rate equation. For example, given the irreversible overall reaction $aA + bB = cC$, the rate equation would be of the following form:

$$-\frac{1}{a}\frac{d[A]}{dt} = -\frac{1}{b}\frac{d[B]}{dt} = \frac{1}{c}\frac{d[C]}{dt} = k[A]^m[B]^n[C]^o$$

where "k" is the rate constant at some experimental temperature. The concentrations (i.e. [A], [B], [C]) are for reaction time, t. Each exponent (m, n, o) may be positive or negative, integer or fraction, or zero. When a reactant or product is not part of the experimentally determined rate equation, its exponent is 0 and its concentration term drops out. The sum of the exponents is the reaction order for the reaction.

Intuitively, the reaction rate would depend on the concentrations of the reactants (i.e. A and/or B) but not the product C. While frequently true, there are documented cases where the rate equation does depend on products. For example, the rate equation for ozone (O_3) conversion to

oxygen is the following (p. 8 of 51):

$$2O_3 = 3O_2 \qquad \frac{1}{3}\frac{d[O_2]}{dt} = -\frac{1}{2}\frac{d[O_3]}{dt} = k[O_3]^2\,[O_2]^{-1}$$

Oxygen is part of the rate equation because it is part of the mechanism:

$$O_3 = O_2 + O \qquad \text{Fast, reversible}$$

$$O + O_3 = 2O_2 \qquad \text{Slow, rate-limiting}$$

How can the rate equation and the mechanism be determined? These are determined through (1) mechanism modeling, 2) theoretical prediction of relative reaction rates, (3) detailed rate experimentation, and (4) measurement of reaction intermediate compounds. Kinetic experimentation will not be discussed in this report.

The important point to remember is that the rate equation cannot be predicted from the overall chemical equations used for thermodynamic evaluations. For example, the following acid dissolution of $Co(NH_3)_6^{3+}$ is strongly favored but requires heat and many hours to see the cobalt chloro complex:

$$Co(NH_3)_6^{3+} + H^+ + Cl^- = Co(NH_3)_5Cl^{2+} + NH_4^+$$

The primary reason for this is that the overall rate of a chemical reaction is determined by the rate-limiting elementary reaction step in a sequence that is only summarized by the overall reaction equation. By comparison, a thermodynamic evaluation only concerns the overall reaction, which only concerns the energy states of the reactants and products. Perhaps the most challenging task of a geochemical kinetic study is the determination of these mechanisms. A kineticist must be concerned with (1) all the elementary steps between reactants and products, (2) their relative rates, and (3) certainly the rate of the

rate-limiting step (i.e. slowest for sequential step mechanisms and fastest for parallel step mechanisms).

Fortunately, one can refer to prior research in which individual reactions, representative of a class of similar reactions, can be generalized into a mechanism model for untested reactions in that class. In the next section, current mechanistic models for mineral leaching will be reviewed. One important premise in kinetics is that the rate for each elementary reaction is only proportional to the concentrations of all reactants for that specific elementary reaction.

Activated Complex Theory

Additional insight and information regarding a geochemical reaction can be obtained through application of the familiar activated complex theory or transition state theory of chemical kinetics (53, 54). The theory is based on three postulates:

1. A metastable "activated complex" is formed from reactants that possesses a higher potential energy than either reactants or reaction products.
2. The number of activated complexes is in statistical equilibrium with the reactants.
3. The reaction rate equals the concentration of the activated complexes times the decomposition rate of the activated complex.

Figure 4 gives a representation of some of these activated complex theory postulates in the form of a potential energy vs. reaction coordinate diagram for a transition metal ligand substitution proceeding by a dissociative mechanism ($[MX]^{n+} + Y^- = MY$). The activated complex theory can be expressed in terms of stable chemical reactants as follows:

$$\text{rate} = \nu[M^+] = k^*[MX][Y]$$

where ν = decomposition rate of activated complex

$[M^+]$ = concentration of the metal activated complex, $[M(H_2O)_5]^{n-1}$

k^* = reaction rate constant

$[Y]$ = concentration of entering ligand Y^-

$[MX]$ = concentration of original metal complex, $[M(H_2O)_5X]^{n+}$

The rate constant, k^*, can be related to thermodynamic parameters of the activated complex:

$$k^* = B(T)\ e^{\Delta S+/R}\ e^{-\Delta H+/RT}$$

where $B(T)$ = term dependent on absolute temperature

$^{\Delta S+}$ = entropy of activation

$^{\Delta H+}$ = enthalpy of activation

R = gas constant

T = absolute temperature

It is useful to compare k^* with the Arrhenius equation, which was derived in 1889 to explain the experimentally observed temperature dependence of chemical reaction rate constants, k:

$$k = A\ e^{-Ea/RT}$$

where A = Arrhenius constant

E_a = activation energy

First, enthalpy of activation is related to experimental activation energy for liquid phase reactions: $\Delta H^+ = E_a - RT$. Second, the Arrhenius constant is related to both temperature and entropy according to $A = B(T)\ e^{\Delta S+/R}$.

A knowledge of the E_a of a geochemical reaction can provide useful clues regarding the mechanism of the reaction as well as its temperature sensitivity (49). For example, geochemical reactions controlled by solution diffusion have E_a values less than 5 kcal/mole while surface-controlled reactions have higher values.

In summary, in geochemical kinetic evaluation the following points are important:

1. Kinetics evaluation operates with a different hypothesis than thermodynamic evaluation - Optimization and selectivity during leaching are based on the relative rates of competing leaching reactions in individual manganese and gangue minerals. By comparison, thermodynamic evaluation only considers the energy states of the reactants and products that appear in the overall reaction equation.
2. Recent work has suggested that many important geochemical reactions are not at equilibrium or steady-state in normal geologic conditions.
3. Kinetic evaluation (rates and mechanisms) of geochemical reactions is much more complex than thermodynamic evaluation.
4. A wealth of information can be obtained about a geochemical reaction from a kinetic evaluation.

Current Mineral Leaching Models

An essential part of the kinetics evaluation of a geochemical reaction is determination of the mechanism of the reaction. The

starting point in this endeavor is the study of previous work on mechanistic models for related reactions. From the viewpoint of geochemical characterization it is useful to review current models of mineral dissolution that emphasize the chemistry at the lixiviant-mineral interface; that is, a molecular view of chemical bond breaking and inorganic solution chemistry. Therefore, the mineral and metal dissolution models from the metallurgy discipline will not be discussed in detail, but can be studied further by reading the text by Habashi (55) or other metallurgy books.

There are two geochemical leaching models, drawn from the theoretical and experimental efforts of two different but related technical disciplines, that summarize the state-of-knowledge regarding mineral leaching kinetics: (1) the surface energy model and (2) the surface coordination model.

Surface Energy Model

The surface energy model for mineral leaching is the general model for crystal growth and dissolution under natural conditions such as weathering (17, 56). It was developed to explain field observations in mineralogy and to predict future trends. In the surface energy model, dissolution preferentially occurs at those points on the mineral surface that possess the highest surface energy. Three principle factors determine surface energy for a point at the mineral surface: (1) the number of chemical bonds the atoms has with the mineral lattice, (2) the presence of point defects (i.e. absence of lattice atoms or presence of impurity atoms), and (3) the presence or absence of crystal dislocation strain energy at that atom.

At a given time, a real crystal surface will contain a number of surface defects such as steps and kinks. For example, lattice atoms which form steps have two faces exposed to the liquid and one less chemical bond to the crystal lattice than planar surface atoms. This means they will possess a higher surface energy than those planar surface atoms. Atoms at the edge of steps form a kink. They have three exposed faces, two fewer bonds than surface atoms, and proportionally higher surface energy than either surface or step atoms. Figure 5, adapted from Blum and Lasaga (57) depicts these structural features for an ideal crystal. Thermodynamically, dissolution for an ideal crystal is favored as follows: kink > step > surface atoms. In general, surface defect sites will have higher surface energies than surface atom sites.

In addition, crystals are rarely ideally structured. They possess lattice offsets called dislocations. Dislocations strain the bonds of the affected atoms, creating highest dislocation strain energy at the atoms that have bonds which are strained the most. This dislocation strain energy adds to the surface energy of any affected surface atoms and would enhance their thermodynamic tendency toward release (i.e. dissolution) from the crystal.

Blum and Lasaga have reported an elegant Monte Carlo simulation of the rates of surface reactions by combining the basic surface energy model with the activated complex theory (57). They determined crystal growth or dissolution for various model crystals by randomly selecting sites and determining the probability of the elementary processes of precipitation, dissolution, and surface diffusion. In related work,

Schott and coworkers (58) recently reported that calcite crystals, under strain to create more dislocations, did dissolve more rapidly than unstrained crystals.

Surface Coordination Model

The surface coordination model for mineral leaching has its origin in inorganic coordination chemistry rather than mineralogy. This model has been largely developed by Stumm (59) and Morgan (60) and their respective aquatic chemistry research groups. It is based on the principle that mineral dissolution is regulated by formation of specific coordination complexes at the mineral surface.

Using a surface coordination model, Stumm and coworkers (59) have treated dissolution of metal oxides and Al silicates like any heterogeneous chemical reaction mechanism which consists of the four steps listed in table 10. The most important chemical reactions in this mechanism are (1) the adsorption of reactant molecules or atoms at the highest energy mineral surface sites and (2) the detachment of the metal atoms from the mineral surface. Generally, the rate-limiting step in this mechanism is considered to be the metal-detachment reaction step.

Adsorption of Reactant Molecules

Initially, adsorption of solution-phase molecules onto mineral surfaces was treated as a physical adsorption phenomenon characterized by the electrostatic Gouy-Chapman-Stern model (61). Recent mineral dissolution experimental data, however, shows adsorption to be more site-selective and thus cannot be explained solely through electrostatics (62). Instead, the adsorption behavior is explained on the basis of a variety of reversible chemisorption (i.e. chemical

bonding) reactions of solution species to specific mineral surface sites. These specific chemisorption reactions have been treated as a series of inorganic chemistry reactions. A link with the surface energy model is that these chemisorption reactions occur more rapidly at surface defects.

Experimentation by Stumm and others (63, 64, 59) have revealed two key chemisorption reaction types that affect metal oxide and Al silicate dissolution:

1. Reversible H^+ bonding at O^{2-} sites to form OH^- and H_2O, thereby weakening metal-oxygen bonds.
2. Coordinate covalent bonding of OH^- and other Lewis base ligands at metal bonding sites, to the extent of replacing weakened metal-oxygen bonds.

Detachment of Metal Species

Detachment occurs when adsorption-altered surface metal atoms have enough weakened metal-oxygen bonds to permit metal release into the solution. Such a phenomenon is termed proton-promoted or ligand-promoted dissolution.

As an example of ligand-promoted dissolution, Furrer and Stumm (63) showed the variations in dissolution rates of δ-Al_2O_3 (k_{ligand}) for two structurally homologous ligand series:

1. $k_{oxalate} > k_{malonate} > k_{succinate}$
2. $k_{salicylate} > k_{phthalate} >> k_{benzoate}$

They proposed a three-step reaction mechanism for these reactions which is summarized in figure 6, adapted from Furrer and Stumm (63). First, there is rapid adsorption of solution ligands in the form of strong

surface [Al^{3+}-ligand] coordination complexes which weakens Al-O bonds. Second, the [Al^{3+}-ligand] complex breaks the Al-O bonds and detaches to form a soluble complex. This is considered to be the rate-determining step. Third, fast protonation occurs to neutralize the excess negative surface charge left by the detached Al^{3+} complex.

The complexes formed in the case of the two structurally homologous ligand series are chelate complexes of differing ring size as shown in figure 7, adapted from Furrer and Stumm (63). It is well accepted that five-atom chelate rings form the most stable complexes, followed by six-atom rings, and then seven-atom rings (6). Four-atom rings and rings composed of eight or more atoms are unusual. Stability of surface complexes is important because it increases the number of potential sites for metal detachment, given a certain ligand concentration and can account for the changes in δ-Al_2O_3 dissolution rates. Furrer and Stumm (63) demonstrated that δ-Al_2O_3 dissolution rate constants increase with ring stability for both series of organic chelators and thus ascribe the basis of the sequence of increasing rate constant values in each structurally homologous ligand series to an increase in relative thermodynamic stability of the [Al^{3+}-ligand] complexes formed.

Reductive Dissolution

Stone and Morgan have extended the surface coordination model to include reductive dissolution (reduction of metal centers) as part of mineral leaching (60, 65, 66). This adaptation of the surface coordination model can be used to explain the mechanism of leaching of many manganese, iron, cobalt, and nickel oxide minerals. For example, Mn^{4+} or Mn^{3+} centers found in the manganese oxide minerals in key U.S.

manganese deposits (table 4) must undergo reduction to Mn^{2+}, the only lower manganese oxidation state that is chemically stable and soluble in water (45).

By incorporating an electron-transfer reaction such as reduction at the mineral surface, the surface coordination model is made more complex. Table 11 summarizes the six reaction steps of the surface coordination model when the reduction dissolution mechanism is incorporated.

In order to understand the possible pathways for the electron-transfer reaction involved in reductive dissolution, Stone and Morgan used the theory of electron-transfer for solution inorganic complexes (6). Electron transfer in solution can occur by two general mechanisms: (1) outer-sphere or (2) inner-sphere.

Outer-Sphere Electron Transfer

Outer-sphere electron transfer occurs when the oxidant and reductant approach each other within some internuclear distance but do not form a covalent bond between each other. When they are closely arranged to permit rapid transfer of electrons from the reductant to the oxidant this arrangement is called an outer-sphere precursor complex. Outer-sphere electron transfer will most readily occur when both the reductant and oxidant undergo ligand substitution very slowly (i.e. they are substitution inert). For example, both $[Fe^{2+}(CN)_6]^{4-}$ and $[Ir^{4+}Cl_6]^{2-}$ are substitution inert with reaction half-lives greater than 1 minute. However, the following one-electron transfer reaction has a half-life of approximately 10^{-5} second:

$$[Fe^{2+}(CN)_6]^{4-} \text{ and } [Ir^{4+}Cl_6]^{2-} = [Fe^{3+}(CN)_6]^{3-} \text{ and } [Ir^{3+}Cl_6]^{3-}$$

Clearly, electron transfer occurs well before any chemical bonding (i.e. ligand substitution of CN^- to Ir^{4+} or Cl^- to Fe^{3+}).

Inner-Sphere Electron Transfer

Inner-sphere electron transfer requires bonding and actually occurs through a ligand simultaneously bonded to both the oxidant and the reductant prior to electron transfer. This common ligand arrangement is called an inner-sphere precursor complex. The mechanism is also called ligand-bridge electron transfer.

Inner-sphere electron transfer reactions were demonstrated by the pioneering studies of Taube and coworkers (67). In this work, they reacted inert Co^{3+} complexes with labile Cr^{2+} complexes to form labile Co^{2+} products and inert Cr^{3+} products. The formation of these products could only be due to transfer of a bridging Cl^- ligand as part of the following electron transfer reaction:

$$Cr^{2+}(H_2O)_6 + Co^{3+}(NH_3)_5Cl \rightarrow [\ (H_2O)_5Cr^{2+}\text{-}Cl\text{-}Co^{3+}(NH_3)_5\ ]$$

precursor

|

| electron transfer

V

$$Cr^{3+}(H_2O)_5Cl + Co^{2+}(NH_3)_5(H_2O)$$

From the above treatment, it follows that there are several requirements necessary for an inner-sphere electron transfer to occur. First, at least one of the reactants must be substitution-labile enough to permit formation of an inner-sphere precursor complex before outer-sphere electron transfer can occur. Second, there must be a suitable (usually weak field) bridging ligand available from either the

reductant or oxidant. Stone and Morgan note that either inner-sphere or outer-sphere electron transfer is possible at mineral surfaces. Just as in solution-phase electron transfer, the choice of mechanism will depend on the ability of solution-phase reductant molecules to form one of the precursor complexes at the mineral surface active sites.

Reductive Dissolution

Stone and Morgan (60), developed a general rate equation for dissolution of metal oxides in natural waters with organic acid reductants present:

$$d[Me^{2+}]/dt = k_2 S_T \frac{\{ k_1[HA] \}}{\{k_1[HA] + k_{-1} + k_2\}} \{1 - \exp(-(k_1[HA] + k_{-1} + k_2)t)\}$$

where: S_T = total moles of mineral surface sites per L solution

$[HA]$ = concentration of reductant, moles L^{-1}

k_1 = rate constant for reductant adsorption, L $mole^{-1}$ min^{-1}

k_{-1} = rate constant for reductant desorption, min^{-1}

k_2 = rate constant for electron transfer, min^{-1}

This rate equation is based on their model for reductive dissolution, which is summarized in table 11 and based on the assumption that the slowest (i.e. rate-limiting) step is either (1) reductant adsorption to form a precursor complex for electron transfer or (2) electron transfer itself, the most common cases found by their research. Once electron transfer has occurred at a given site, the new products rapidly leave the mineral surface.

Stone's earlier work (65, 66) studied reductive dissolution of feitknechtite (β-MnOOH) with 27 aromatic and nonaromatic compounds that model natural organics in waters. This work supported the general reductive dissolution mechanism. For organic compounds capable of 2-

electron transfer, the following rate equation was found at constant pH:

$$d[Mn^{2+}]/dt = k_x [\text{Reductant}] ([MnO_x]_{initial} - [Mn^{2+}])$$

where: $[Mn^{2+}]$ = solution concentration of Mn^{2+} with time, mole L^{-1}

k_x = rate constant, L $mole^{-1}$ min^{-1}

There were two additional results from this work. First, relative changes in dissolution rates did not correspond to the changes in free energy of the overall reaction for given reductants. Second, the most important factor in determining relative dissolution rates was the tendency of the reductant to form complexes at the mineral surface, i.e., dissolution rates were fastest for those reductants which were also the strongest potential ligands.

Recent work by Laha and Luthy (68) have confirmed Stone's mechanism and rate equation for the reaction of anilines and other aromatic reductants with δ-MnO_2.

Combined Surface Energy and Surface Coordination Model

Lastly, Wieland, Wehrli, and Stumm (69) combined the surface coordination model with the surface energy model through the activated complex theory (ACT) to develop a single general rate equation for proton- and ligand-promoted mineral dissolution:

$$\text{Dissolution Rate} = R = k\, x_a\, P_j\, S$$

where: R = dissolution rate, moles m^{-2} sec^{-1}

k = rate constant, sec^{-1}

x_a = mole fraction of surface sites active to dissolution (defects, steps, kinks etc.)

P_j = probability a specific site will form a precursor complex

S = surface density of total crystallographic sites, moles m^{-2}

They were able to apply the rate equation to interpret literature kinetic data for proton-promoted dissolution of mineral oxides and silicates. They used an experimental Freundlich adsorption isotherm to estimate x_a, a Bragg-Williams lattice statistic to approximate P_j, as well as literature-reported data for the rate constants (k) and the surface densities of active sites (S). Note that this rate equation incorporates both the surface energy model parameter (S) and the surface coordination model parameters (x_a, P_j).

In summary, two mineral leaching models, (1) the surface energy model and (2) the surface coordination model were developed in the past decade to explain much of the available experimental kinetic data. The work by Stone and Morgan on reductive dissolution of manganese oxides is particularly relevant to in situ leaching of key U.S. manganese ore deposits. Recent work by Stumm and coworkers (69) has focused on combining the models with the activated complex theory to develop a general rate equation for proton- and ligand-promoted mineral leaching kinetics. The recent review by Stumm and Wollast (70) provides an excellent review of mineral dissociation models.

Chemical Bonding and Methods to Predict Leaching Reactivity

Since detailed experimental research to determine the leaching kinetics of a given manganese mineral by a lixiviant is time-consuming and expensive, it would be highly desirable to utilize the potential of theoretical chemistry methods for predicting the leaching ability of

promising lixiviants. A preliminary evaluation could speed lixiviant development time by optimizing the experimental efforts.

If mineral leaching can be viewed as a heterogeneous chemical reaction that obeys kinetics of inorganic solution chemistry, then useful theoretical methods to predict mineral reactivity (e.g. leaching rates) are available. This view seems reasonable since the structure and reactivity of minerals are based on the same fundamental atomic properties that govern structure and reactivity for inorganic complexes in solution (71, 72):

* size and charge of ions and atoms
* configuration of valence electrons
* chemical bond strengths
* chemical bond polarity
* spatial symmetry of chemical bonds

It should be noted that chemical reactivity in gases, liquids, and solids involves the creating or breaking of chemical bonds between atoms and ions. In the case of mineral leaching, bond breaking occurs at the solid-liquid interface.

Chemical Bonding

One way to compare structure and reactivity between manganese minerals and solution complexes is to review how manganese minerals and complexes are bonded (71). The highly symmetric structure and associated chemical properties of many metal minerals including manganese minerals are primarily the result of two types of chemical bonding: (1) ionic and (2) covalent.

Ionic Bonding

Ionic bonding is the electrostatic attraction of oppositely charged ions at a distance where attractive forces are balanced by coulombic repulsions of valence electron shells. Ionic bonding occurs between cations and anions with filled outermost electron shells. For metals (cations) and most anions, ionic bonding leads to highly symmetric close packing of alternating cations and anions in three-dimensional arrays. For nearly pure ionic minerals (i.e. NaCl), the structure depends on the ratio of the ionic radii of the cation (r_+) and anion (r_-). The ratio of ionic radii, r_+/r_-, determines the coordination number, i.e., the number of neighboring ions of opposite charge that can surround each ion. Table 12 summarizes the required r_+/r_- ratio for common mineral structures.

The strength of the ionic bonds is represented by the lattice energy (U), which can be calculated from the Born-Lande' equation:

$$Metal_mX_x\ (s) = mMetal^{z+}\ (g) + xX^{z-}\ (g)$$

$$U = \frac{N_A M z^+ z^- e^2}{4 \pi \epsilon_o r_o} [1 - 1/n]$$

where: U = lattice energy, Joule $mole^{-1}$

N_A = Avogadro's number, 6.022×10^{23} $mole^{-1}$

M = Madelung constant for lattice structure symmetry

z^+ = charge of cation

z^- = charge of anion

e = electron charge, 1.602×10^{-19} coulomb

ϵ_o = vac. dielectric constant, 8.854×10^{-12} $coulomb^2$ $meter^{-1}$ $Joule^{-1}$

r_o = distance between cation and anion, meter

n = Born exponent, filled electron shell repulsions

With constants substituted, the equation can be reduced to the following:

$$U = \frac{1.389 \times 10^{-4} \; M \; z^+ \; z^-}{r_o} \; [\, 1 - 1/n] \quad \text{Joule mole}^{-1}$$

Values for the M, r_o, and n are experimentally determined and can be obtained from standard mineralogy texts (71). The value for n is the average of n_{anion} and n_{cation}. For NaCl, U is calculated to be -765 kJ $mole^{-1}$.

Given: M = 1.747

z^+ = +1

z^- = -1

r_o = 2.82×10^{-10} meter

n = 9.1

Ionic bonding in solution is similar to that in a mineral in that cations and anions will again approach one another, displacing some or all of the solvent molecules between them, until they achieve electrostatic equilibria. Such complexes are called ion pairs or outer-sphere complexes. Unlike mineral lattices, ion pairs continue to dissociate and reform in solution because there is considerable motion within a liquid and largely absent inside a mineral.

Although ionic bonding is the most important type of chemical bonding in many minerals, few contain purely ionic bonds (71, 72). Frequently, some degree of covalent bonding (i.e. sharing of valence electrons) is part of the mineral lattice bonds.

Covalent Bonding

Covalent bonding is so central to traditional chemistry theory and practice, that only the comparison between mineral chemical bonding and solution inorganic chemical bonding will be discussed here. Inorganic chemistry texts by Cotton and Wilkinson (6, 45), Jolly (72), or others contain excellent reviews of covalent bonding and its significance to gaseous, liquid, and solid phase inorganic chemistry.

As with ionic bonding, the nature of covalent bonding determines the structure and reactivity of minerals and solution complexes. One important characteristic of covalent bonding that contrasts with ionic bonding is that covalent bonding is highly directional, with the strongest electron density occurring in direct lines or planes between the cation and anion.

An atom (ion) will tend to form covalent bonds to fill its outermost electron energy shell. Thus, the tendency to form covalent bonds, the spatial symmetry of the covalent bonds formed, and the energy of covalent bonds formed are all related to the electron configuration of the atom (ion). This aspect of covalent bonding was first embodied in the familiar Lewis octet theory. Furthermore, the bonding orbitals (s, p or d) for a given atom will mix to form hybridized orbitals that will be separated in 3-dimensional space to maximize the distance between them. This concept is the familiar valence-shell electron pair repulsion (VSEPR) theory. The result is a correlation between the number of covalent bonds an atom tends to form and the resulting spatial symmetry of the resulting complex (table 13). The Lewis and VSEPR

theories characterize the nature of most non-transition metal bonding cases.

Ligand Field Theory

A covalent bonding model specifically for transition metals was developed called the ligand field theory. This simple model begins with the crystal field model - a transition metal with six negative point charges around it at octahedral positions. Initially, the energy of the five d orbitals are equal, i.e. degenerate. As charges are brought closer to the metal, the 3d orbital energies change to produce three orbitals with lower energies (t_{2g}) and two with higher energies (e_g). A similar treatment for four charges placed at tetrahedral positions results in splitting the d orbitals into a reverse set of three higher (t_2) and two lower (e) orbitals. Figure 8, adapted from Cotton et.al. (6), is an energy diagram for crystal field splitting of the d orbitals. The magnitude of the splitting for actual complexes varies with ligand and metal. In many cases, the electronic energy of the metal is lowered when the five d orbitals are split. This energy reduction is called the ligand field stabilization energy.

The ligand field theory has explained much of the experimental structural, magnetic and spectroscopic properties for first-row transition metals. It has also been helpful is predicting the reactivity of transition metals. Despite the enormous success of ligand field theory, it is not a complete treatment of metal-ligand bonding since it only deals with the d orbitals of the metal.

Molecular Orbital Theory

To explain more complex bonding and other chemical properties, a more general theory for covalent bonding known as the molecular orbital theory (MOT) has been developed. The basic premise of MOT is that bonding between atoms occurs when their atomic orbitals overlap to concentrate electron density between their nuclei. This concentration of electron density is called a molecular orbital. For a set of atoms (ions), one uses a knowledge of the spatial symmetry and energy of atomic bonding orbitals to predict formation of new molecular bonds in a chemical reaction. Orbital interactions can be classified into three categories: (1) bonding, leading to lower energy and stabilization, (2) antibonding, leading to higher energy and destabilization, and (3) nonbonding with no significant change in energy. Bonding and antibonding molecular orbitals possess specific spatial symmetries that reflect the types of atomic orbitals involved: (1) sigma (σ), s and p_z (2) pi (π), similar p_y or p_z, and (3) delta (δ), d. Figure 9, adapted from Cotton et.al. (6), shows the spatial symmetry characteristics of simple σ and π molecular orbitals.

In solution, the structure and reactivity of manganese and other first-row transition metals are dominated by covalent bonding and the arrangements of valence electrons in their unfilled 3d shells. When 4 to 7 electrons are in the 3d shell, the electrons will either be highly paired (i.e. low spin) or unpaired (i.e. high spin). Due to low ionization potentials, these metals frequently exist as 2+ or higher oxidation state cations. The metals will tend to fill the 3d inner coordination shell by bonding with ligands that can donate one or two

electrons to a given covalent bond. The case where an anion donates both electrons is called a coordinate covalent bond.

For relatively simple metal complexes, MOT can be applied to predict reactivity. For example, the simple but common case of σ-only coordinate bonding of six ligands (L) to some transition metal (M) to form ML_6 has been derived. Figure 10, adapted from Cotton et.al. (6), summarizes the six sets of metal and ligand bonding configurations that lead to six σ bonds. Figure 11 is an energy diagram for this case and includes all bonding, nonbonding, and antibonding energy states. Comparison of the results in figures 8 and 11 shows that ligand field theory and MOT are compatible for this case as both predict the same splitting of d orbitals. However, only MOT accounted for all possible molecular orbitals.

Since all the bonding theories discussed above are based on fundamental atomic properties, the structural and reactivity consequences for ionic and covalent bonding should apply for solid (e.g. minerals), liquid, or gas phases. This means that the predictive methods for chemical reactivity for aqueous metal complexes should be useful for mineral leaching reactions.

Manganese Bonding Structures

To determine if the predictive methods for chemical reactivity for aqueous manganese complexes are useful for predicting manganese mineral leaching reactions, it is necessary to compare the structure and bonding features of manganese both in solution and in mineral lattices. Experimental evidence has shown that in oxygenated water, manganese is most stable as the Mn^{2+} ion, which has five unpaired 3d electrons (high

spin) and forms coordinate covalent bonds with six ligand sites in octahedral bonding symmetry (45). This was also predicted by the MOT treatment of the simple ML_6 bonding case shown in figure 11. When the resulting Mn^{2+} complex is charged, i.e. $[Mn(H_2O)_6]^{2+}$, it could form ion pairs with appropriate counter ions, ($[Mn(H_2O)_6]^{2+}$, $SO_4^{=}$).

The spatial symmetry for manganese in key manganese minerals has already been characterized in prior crystallography work. The data in table 4 shows that manganese has octahedral symmetry with a metal coordination number of 6 for all three oxidation states (4+, 3+, 2+), except that Mn^{2+} in hausmannite has 4-coordinate tetrahedral symmetry. Metal centers at edge or kink positions on the mineral surface will have H_2O, OH^-, or other common anions at their non-lattice bonding positions.

What type of chemical bonding would be expected for manganese minerals? For the most important group (i.e. manganese oxides), ionic bonding predominates. This is expected since the anion, $O^{=}$, has a complete outer electron shell (6). Calculation of the ionic radii ratios (r_+/r_-) for $O^{=}$ with Mn^{4+}, Mn^{3+}, or Mn^{2+} (table 14) confirms the tendency shown in table 4 toward octahedral symmetry during ionic bonding. The ionic radii ratio for Mn^{4+} was only slightly below the minimum ratio required for octahedral symmetry. For rhodochrosite ($MnCO_3$), the carbonate anion also has a closed outer electron shell and ionic bonding is dominant. The $CO_3^{=}$ anions are centered at the octahedral bonding positions of the Mn^{2+} metal centers (71). For rhodonite ($MnSiO_3$), the Mn^{2+} cations have oxygens from SiO_4 groups at their octahedral bonding positions (71). These oxygens are covalently

bonded to Si and have a complete outer electron shell. Again, ionic bonding is significant.

However, Zoltai and Stout (71) have emphasized that the bonding in many mineral lattices also has a covalent bonding component. They have suggested that electronegativity can be used as a guide to determine the predominant bonding type. Electronegativity (χ) is a fundamental property of atoms and is defined as the power of the atom to attract electrons to it (72). When the electronegativity difference between the cation and anion of a mineral bond is great, i.e., $\chi_O - \chi_{Fe} = 1.9$, the bond will tend to be mostly ionic. Likewise, a lesser electronegativity difference, i.e., $\chi_S - \chi_{Fe} = 0.8$ means that some covalent bonding will be present. For the important Mn-O bond, the electronegativity difference is 1.9, suggesting strong ionic bonding.

During dissolution at a mineral-solution interface, the chemical environment becomes a mixture of mineral lattice bonding and solution-phase bonding. For example, the Mn atoms on edge and kink sites will have either two or three of its six bonding positions exposed to the solution, respectively. It is reasonable to treat these positions as solution rather than mineral lattice bonding positions. Since all three Mn centers (Mn^{4+}, Mn^{3+}, or Mn^{2+}) have unfilled 3d orbitals with varying numbers of 3^d electrons (3, 4, 5 respectively), one would expect octahedral covalent bonding at the exposed bonding sites of manganese minerals.

In summary, ionic bonding predominates in the lattice bonding for key manganese minerals. However, at mineral-solution interfaces, exposed octahedral bonding positions about Mn centers should behave like

those of solution-phase Mn coordinate covalent complexes. Therefore, theoretical methods to predict chemical reactivity of solution-phase Mn complexes can be applied to mineral surface reactions, including dissolution. Note that the reductive dissolution model for transition metal oxide leaching involves both (1) chemisorption, a heterogeneous ligand substitution reaction, and (2) reduction of metal by the chemisorbed ligand.

Leaching Reactivity Predictive Methods

There are four theoretical methods for predicting the relative ease that transition metal chemical reactions will occur at the mineral-liquid interface:

1. General rules for metal substitution reactivity
2. Ligand field theory with activated complex theory
3. Molecular orbital theory
4. Linear free energy relationships (LFER)

In the next section the first three will be applied to the test case of this report - characterization of SO_2 batch leaching of the key U.S. manganese minerals (table 4) as reported by Pahlman and Khalafalla (8).

General Rules for Metal Substitution Reactivity

The three general rules for solution-phase ligand substitution reactivity of metals are listed in table 15. The application of these rules was developed to explain experimental results in a general way and have been summarized by Jolly (72). For example, experimental evidence has shown that Co^{2+} undergoes rapid substitution of NH_3 while Co^{3+} reacts slowly (i.e. inert). Rule 3 from table 15 supports these results

because Co^{2+} is a d^7 metal (labile) and Co^{3+} with is low-spin d^6 (inert) with NH_3.

Ligand Field Theory with Activated Complex Theory

The application of ligand field theory combined with the activated complex theory (ACT) was developed to estimate the activation energies for prospective substitution reactions. This method was pioneered by Basolo and Pearson (74) and is also summarized by Jolly (72). This method requires a knowledge of the mechanism of a given type of substitution reaction, in particular the structure and coordination of the activated complex.

With the knowledge that solution octahedral transition metal complexes form either 5-coordinate or 7-coordinate activated complexes, Basolo and Pearson calculated the energy changes for these possible complexes based solely on changes in the ligand field stabilization energies between the reactant complex and activated complex. This method was a more rigorous utilization of the knowledge of the time (mid-1960's) with regard to (1) chemical kinetics, (2) mechanisms for transition metal substitution reactions, and (3) inorganic covalent bonding. Interestingly, this approach reached the same predictions as the qualitative rules above, except d^8 metals were predicted to form inert complexes, especially square planar ones.

Molecular Orbit Theory

Application of molecular orbital theory (MOT) was developed to identify favorable bonding conditions for mineral surface reactions, including electron transfer. This exciting new predictive method has

been pioneered by George Luther, who has used the MOT approach in studying several important geochemical redox reactions (75, 76).

When two molecules meet, covalent bonding or electron transfer occurs when electron density can flow from the highest occupied molecular orbital (HOMO) of a donor (base) molecule to the lowest unoccupied molecular orbital (LUMO) of an acceptor (acid) molecule. Based on this central principle, the following conditions must be met for electron density to flow (75):

1. Molecular or atomic orbitals must have similar spatial symmetry for positive orbital overlap. For example, alignment of an s orbital from one molecule with a p_z orbital from another orbital to form a potential σ molecular orbital.
2. The energy of the HOMO for the donor molecule must be greater than but similar to the LUMO for the acceptor molecule. Best results occur when the energy of the LUMO is within 6 eV/molecule (i.e. 579 kJ $mole^{-1}$) of the energy of the HOMO.
3. The bonds made or broken must be consistent with expected product compounds for the proposed reaction.

When the above conditions are met, a given reaction is called symmetry allowed and should rapidly take place (i.e. labile reactivity).

An excellent example of this MOT method is Luther's explanation for rapid reduction of MnO_2 by HS^- (76), a reduction reaction which was reported to be rapid by Burdige and Nealson (77). Since the Mn^{4+} metal center of MnO_2 has a $3d^3$ electron configuration, it is inert to most ligand substitution reactions. In this case, however, the $3p_z$ orbital of HS^- can form a σ bond with the $3d_{z2}$ orbital of the Mn^{4+} (Figure 12,

adapted from Luther (76)). Overlap symmetry is good and the energies of the $3p_z$ and $3d_{z2}$ orbitals are comparable. Therefore, a rapid 2-electron transfer can be made from HS^- to the unoccupied $3d_{z2}$ and or $3d_{x2-y2}$ of Mn^{4+}, creating a Mn^{2+} mineral center and rapid breakdown of the surrounding Mn-O lattice bonding.

Linear Free Energy Relationships

The application of the concept of linear free energy relationships (LFERs) was developed to predict reactivity of prospective mineral-lixiviant systems based on experimental data for similar reactions. The LFER concept is based on the principle that changes in free energy of activation for a series of related chemical reactions is proportional to changes in the free energy properties of ground-state products. From this relationship the following basic form for LFERs can be derived:

$$\ln(k_1/k_2) = \beta \ln(\Delta G_1^\circ/\Delta G_2^\circ) = \beta \ln(K_1/K_2)$$

where: k_n = rate constants for n-th reaction

β = proportionality constant

ΔG_n° = free energy of n-th reaction

K_n = stability constant for n-th reaction

The use of LFERs has found wide application in organic chemistry kinetic studies where there are a number of reactions involving homologous reactant series (53, 78). The Swain-Scott and Edwards LFER equations for organic chemistry nucleophilic (anionic) substitution reactions are mechanistically similar to anionic complexation of transition metals. The Edwards equation has the following form:

$$\log (k/k_o) = \alpha E_n + \beta H$$

where: k = rate of unknown reaction

k_o = rate of known reaction

α = sensitivity of reaction to reagent nucleophilicity

E_n = nucleophility of reagent

β = sensitivity of reaction to reagent basicity

H = basicity of reagent

An attractive feature for the Edwards equation is that two of the parameters, E_n and H are based on fundamental properties of the reagents. $E_n = E^o + 2.60$, where E^o is the formal potential for the reagent. $H = pK_a + 1.74$, where K_a is the dissociation constant for the conjugate acid of the anionic reagent.

There are recent geochemical applications of LFERs. Wieland et.al. (69) plotted log of experimental rates (R_H) for proton-promoted dissolution of various minerals versus a number of thermodynamic energy parameters and found the best linear correlation was log (R_H) vs. E_M, the Madelung or site energy for the minerals. Laha and Luthy (68) found LFERs for reaction rates of aromatic amine oxidation by δ-MnO_2 with electrochemical half-wave potentials and a Hammett constant.

If a series of mineral reactions can be expected to have the same kinetic mechanism, LFERs would appear to be an excellent predictive method to evaluate untested lixiviant by comparing key thermodynamic properties with lixiviants for which experimental kinetic data is available.

Kinetic Evaluation: SO_2 Leaching of Manganese Ores

The general dissolution rate equation (69) and the kinetic studies by Stone and Morgan (60, 65, 66) on reductive dissolution of manganese oxides provide excellent models for studying the kinetics of in situ leaching of manganese ores.

In this section a kinetic evaluation will be made for the manganese example of this report - SO_2 batch leaching of the key U.S. manganese minerals (table 4) and related gangue (table 9) as reported by Pahlman and Khalafalla (8).

The first three theoretical predictive methods can be used to assess the relative reactivity of SO_2 to leach manganese from the minerals listed in table 4. Since manganese must be in the Mn^{2+} form to be stable and soluble in aqueous lixiviants, the higher oxidation state manganese oxides must be reduced to Mn^{2+} during dissolution:

$$d[Mn^{2+}]/dt = k_x [SO_2] ([MnO_x]_{initial} - [Mn^{2+}])$$

where: $[Mn^{2+}]$ = solution concentration of Mn^{2+} with time, mole L^{-1}

k_x = rate constant, L $mole^{-1}$ min^{-1}

The Stone and Morgan mechanism for reductive dissolution (table 11) includes chemisorption of potential reductants for Mn oxide dissolution. Chemisorption is generally regarded as covalent bonding of solution-phase molecules to the mineral surface. To achieve manganese reduction, the reductant must either (1) directly bond the Mn center for an inner-sphere electron transfer or (2) bond a nearby atom, placing the reductant within a few angstroms of the metal center for an outer-sphere electron transfer.

Application of General Rules and Ligand Field Theory Methods

Since mineral dissolution can often be enhanced by complexation of solution ligands (including H^+) at the mineral surface, general rules for metal substitution reactivity and the ligand field theory can be applied to predict ligand bonding to the manganese centers of minerals. Manganese is a first-row transition metal. Rule 3 of table 15 predicts the following for the oxidation states of manganese found in the minerals:

* Mn^{4+}	$3d^3$	inert
* Mn^{3+}	$3d^4$ (high spin)	labile
* Mn^{2+}	$3d^5$ (high spin)	labile

In contrast, all metal centers of important iron gangue minerals are labile. The center for hematite and goethite is Fe^{3+}, which is $3d^5$, high spin. The center for siderite is $3d^6$, high spin. In addition, Ca^{2+} in minerals is very labile to covalent bonding. It should be noted that neither iron nor calcium gangue minerals require a redox reaction as part of their mineral dissolution process.

Several interesting implications for manganese mineral leaching follow from the above results:

1. The minerals found to be most reactive with SO_2 (i.e. Mn^{4+} oxides pyrolusite and romanechite) are generally substitution inert. This suggests that electron transfer for Mn^{4+} minerals should proceed by an outer-sphere mechanism since covalent bonding with a reductant would not be necessary. For the reductive dissolution mechanism, chemisorption can only facilitate dissolution by bonding reductant molecules near the nonreactive Mn^{4+} metal centers.

2. Since Mn^{3+} is generally labile, electron transfer for hausmannite, manganite, and braunite could occur via an inner-sphere mechanism for reductants capable of forming covalent bonds with Mn^{3+} centers. Since Mn^{3+} minerals need only a one-electron reduction to reach the soluble Mn^{2+} state, one would predict that an SO_2 free radical is formed rather than the $SO_4^=$ formed from a two-electron transfer (hence oxidation) from SO_2.
3. The substitution lability of Mn^{3+} and Mn^{2+} mineral sites support the general proton- or ligand-promoted dissolution model of Stumm and coworkers. One test for this model would be to compare dissolution rates for a representative Mn^{4+}, Mn^{3+}, and Mn^{2+} mineral in the presence of a strong complexing agent.
4. Mn^{3+} complexes formed near the mineral-solution interface will be highly reactive to further ligand substitution and reduction to Mn^{2+}. This will make it difficult to detect Mn^{3+} complexes formed during mineral dissolution.
5. The Mn^{2+} sites of $MnCO_3$ and $MnSiO_3$ do not require reduction and would be labile to chemisorption that would weaken mineral lattice bonding and facilitate mineral leaching. Since the mechanism for leaching Mn^{2+} minerals is different from that for higher valence manganese oxides, selection and optimization of lixiviants for Mn^{2+} manganese mineral leaching will be different.

Application of Molecular Orbital Theory

The general rules for transition metal reactivity were useful to predict the bonding potential of reductants and other solution ligands to exposed manganese mineral centers. Molecular orbital theory (MOT)

can provide predictions about the mechanism and relative rates of SO_2 reduction of Mn^{4+} and Mn^{3+} metal centers. The SO_2 reaction mechanism can be viewed in a manner analogous to that of Luther for HS^- reduction of MnO_2 (76).

First, let us review the general electronic structure and symmetry of the SO_2 molecule. Figure 13 shows the Lewis diagrams for SO_2. The molecule has bent planar symmetry with a 119.5 degree angle between the two O-S bonding axes. Generally, the S-O bonding for SO_2 has been viewed as σ bonding with π resonance bonding as shown in Figure 13. The molecule has been the subject of a recent evaluation by Purser (79), who presented evidence that SO_2 has stable π bonding between S and each O atom.

In addition, it is known from previous experimentation that SO_2 exhibits a range of different bonding symmetries with transition metals, including direct bonding between S and the metal. Some of the most common examples are present in figure 14, which was adapted from Cotton and Wilkinson (45) and Schenk (80).

The MOT application can begin with a qualitative MOT energy diagram of SO_2 (figure 15) based on the work of Gimarc (81). Since both S and O have six electrons in their highest unfilled energy shell, there are 18 valence electrons to place into the 12 molecular orbitals formed by one S atom and two O atoms. As shown in figure 15, this means that the highest occupied molecular orbital (HOMO) for SO_2 is the antibonding (*) π orbital labeled $4a_1$.

How does SO_2 meet the two essential requirements for bonding and electron transfer as described by Luther 76)?

1. Is there favorable overlap symmetry between the HOMO of the electron donor (SO_2) and the LUMO of the acceptor (Mn^{4+} or Mn^{3+}) ?
2. Is the energy of the SO_2 HOMO energy greater than the energy of the LUMOs of Mn^{4+} and Mn^{3+} ?

Regarding orbital overlap, figure 16 shows that SO_2 has an ideal symmetry for bonding and subsequent reduction of Mn^{4+} centers by an inner-sphere electron-transfer mechanism. In a fashion similar to HS^- (figure 12), the z-axis component of the HOMO for SO_2 that originates from the S atom can overlap the vacant $3d_{z2}$ orbital of Mn^{4+}, forming a σ bond along a z-axis of approach.

Regarding orbital energy levels for σ bonding and electron transfer from SO_2 to Mn^{4+}, the energy requirement is also met. According to Luther (76) the estimated energy for HOMO of an atom or molecule is the ionization potential (IP), which is -12.34 eV for SO_2 (82, p. 10-215). The estimated energy for the LUMO of an atom or molecule is the electron affinity (EA) (76), which is -51.2 eV for Mn^{4+} (82, p. 10-210). Therefore, both orbital overlap symmetry and relative energies of the HOMO and LUMO are favorable for z-axis σ bonding between SO_2 and Mn^{4+}.

Once the SO_2 is bonded to the metal center, electrons can be rapidly transferred to the vacant $3d_{z2}$ orbital of Mn^{4+} via an inner-sphere electron-transfer mechanism. This is an interesting prediction because Mn^{4+} is a d^3 system and kinetically inert. Generally, one would predict that an "inert" metal could not form bonds fast enough to promote inner-sphere electron transfer. However, the correct symmetry and favorable energy comparison between the HOMO of SO_2 and LUMO of Mn^{4+} permit labile formation of a σ bond with Mn^{4+} prior to electron transfer.

Figure 17 reveals that a similar inner-sphere mechanism is favorable for one-electron transfer from SO_2 to Mn^{3+} metal centers. The orbital symmetry is the same. The LUMO energy for Mn^{3+} is -33.67 eV versus -12.34 eV for the SO_2 HOMO. Recall that Mn^{3+} is a d^4 high spin and should be labile to σ bonding with SO_2. However, additional activation energy must be expended to unpair the SO_2 $4a_1$ electrons before transferring one electron to Mn^{3+}. This higher activation energy for SO_2 reduction of Mn^{3+} versus Mn^{4+} should translate into a slower reductive dissolution rate for Mn^{3+} versus Mn^{4+} mineral centers.

The overall reductive dissolution mechanism for Mn^{4+} and Mn^{3+} oxides by SO_2 is summarized in figure 18. The favorable molecular orbital symmetry and energy match between SO_2 and the metal centers of manganese oxides result in rapid reductive dissolution of these acid-resistant minerals.

Based on this kinetic evaluation of SO_2 leaching of manganese oxides, we can address the three optimization questions explored earlier during thermodynamic evaluation.

1. What is a geochemical explanation for leaching efficiency differences among the manganese minerals?

Unless, the residence time is long enough, the relative leaching rates of SO_2 with the table 4 manganese minerals will depend on the ability of SO_2 to rapidly bond and reductively dissolve Mn oxides. In particular, SO_2 has the ability to complex and reduce the Mn^{4+} centers of pyrolusite and romanechite by rapid two-electron transfer from SO_2 via a sigma bond to the Mn^{4+} vacant $3e_{g*}$ orbitals. However, Mn^{3+} minerals (i.e. hausmannite, braunite, or manganite) will accept one

electron from SO_2 to reach the water-soluble Mn^{2+} state. These one-electron transfer reactions require a higher activation energy to decouple the two electrons in the HOMO of SO_2 before transferring one electron to the Mn^{3+}. This should result in a slower relative SO_2 reductive dissolution rate for Mn^{3+} minerals than Mn^{4+} minerals.

Leaching of rhodochrosite and rhodonite do not benefit from SO_2 reductive dissolution and require large quantities of H^+ to break mineral lattice bonds via a proton-promoted dissolution mechanism.

2. What can be done to minimize leaching of Ca?

Since calcite proceeds by a proton-promoted dissolution mechanism, SO_2 leaching should be operated at the highest possible pH that still permits SO_2 reduction of manganese oxides. For example, at pH 2 approximately 39 mole % of the total S is present as SO_2. At pH 3 only 5.5 mole % is present as SO_2.

3. What can be done to minimize leaching of Fe ?

Leaching of the key Fe minerals (i.e. hematite, geothite, and siderite) all also proceed by a proton-promoted dissolution mechanism and can be minimized by operating at the highest possible pH.

*** CONCLUSIONS AND RECOMMENDATIONS

Faced with the need to develop highly selective lixiviant systems for in situ leach mining of critical/strategic or precious commodities, this report introduces a geochemical characterization approach to selection and optimization of potential lixiviants. This report represents a first effort to apply geochemical characterization by detailing a theoretical (1) thermodynamic and (2) kinetic evaluation modeling effort. It is important to remember that this theoretical work

must then be followed by appropriate laboratory experimentation to both (1) verify lixiviant reactivity hypotheses and (2) determine intrinsic reaction rates and leaching efficiencies for geochemical modeling and engineering scale-up of promising lixiviant-ore systems.

Geochemical characterization follows geologic characterization of a target ore and consists of both (1) theoretical geochemical modeling and (2) laboratory experimentation of probable mineral surface reactions necessary to leach commodity metals.

Once geologic characterization for a target commodity has been performed, a reasonable geochemical reaction model can be hypothesized and subjected to a theoretical geochemical thermodynamic and kinetic evaluation.

Since the chemical environment at the mineral-solution interface becomes a mixture of mineral lattice bonding and solution-phase bonding, leaching reactivity can be estimated by using predictive methods based on general inorganic chemistry:

1. General rules for metal substitution reactivity
2. Ligand field theory with activated complex theory
3. Molecular orbital theory
4. Linear free energy relationships (LFER)

In this report, the potential of geochemical characterization modeling was demonstrated by evaluating the experimental results of batch leaching of key domestic manganese minerals (table 4) using SO_2 solutions (8). Thermodynamic evaluation revealed that free energies for most SO_2 leaching reactions of the minerals were quite negative (table

8) but not different enough to explain differences in 30-minute leaching efficiencies (table 7).

This result suggested that differences in SO_2 efficiencies may be due to the rate (i.e. kinetics) of individual mineral leaching reactions. A detailed kinetic evaluation revealed the reason why normally inert (i.e. slow reacting) Mn^{4+} oxides such as pyrolusite and romanechite rapidly dissolved. The SO_2 molecule has an ideal molecular structure to covalently bond a Mn^{4+} metal center and rapidly reduce it to water solution Mn^{2+} by a single two-electron transfer reaction. A similar but relatively slower one-electron transfer mechanism permits reductive dissolution of Mn^{3+} oxides. Dissolution of rhodochrosite ($Mn^{2+}CO_3$), rhodonite ($Mn^{2+}SiO_3$), and gangue minerals do not use SO_2 reduction but requires H^+ (i.e. low pH).

Therefore, the thermodynamic and kinetic modeling of geochemical characterization appears to be an efficient approach to preliminary selection and optimization of potential lixiviants for a newly geocharacterized ore body. It can provide a basis for subsequent lab experimentation to develop a highly selective lixiviant system for possible field studies.

It is suggested that geochemical characterization could be further refined and used for development of leach mining lixiviants. The payback of geochemical characterization should be (1) increased commodity leaching selectivity and (2) more focused and expeditious experimental efforts to develop new in situ mining lixiviants.

*** REFERENCES

1. U.S. Department of the Interior. The Mineral Position of the United States--1990. Annual Report of the Secretary of the Interior Under the Mining and Minerals Policy Act of 1970, U.S. Dept. Int., 1990, 120 pp.

2. Staff, U.S. Bureau of Mines, Mining Research Directorate. Issues, Trends, and Needs in the U.S. Mining Industry: A Mining Research Prospective. BuMines, Sept. 1987, 106 pp.

3. U.S. Department of the Interior. Project 2000--A Strategic Plan for the Bureau of Mines. U.S. Dept. Int. July 1985, 163 pp.

4. Staff, U.S. Bureau of Mines. In Situ Leach Mining. BuMines IC 9216, 1989, 107 pp.

5. Pugliese, J. M. and W. C. Larson. Bibliography on In Situ Mining of Metals. In Situ, v. 10, No. 3, 1986, pp. 277-311.

6. Cotton, F., G. Wilkinson, and P. Gaus. Basic Inorganic Chemistry. John Wiley and Sons, 2nd Edition, 1987, 708 pp.

7. Khalafalla, S. E., and J. E. Pahlman. Selective Extraction of Metals from Pacific Sea Nodules with Dissolved Sulfur Dioxide. BuMines RI 8518, 1981, 26 pp.

8. Pahlman, J. E., and S. E. Khalafalla. Leaching of Domestic Manganese Ores with Dissolved SO_2. BuMines RI 9150, 1988, 15 pp.

9. Olson, G. J., and R. M. Kelly. Microbiological Metal Transformations - Biotechnological Application and Potential. Biotech. Progress, V. 2, No. 1, 1986, pp 1-15.

10. Decker, R. F. Biotechnology/Materials: The Growing Interface. Metall. Trans. A., v. 17A, Jan. 1986, pp. 5-30.

11. Brinckman, F. E., and G. J. Olson. Chemical Principles Underlying Bioleaching of Metals From Ores and Solid Wastes, and Bioaccumulation of Metals from Solutions. Biotechnology and Bioengineering Symp., No. 16, John Wiley and Sons, 1986, pp. 35-44.

12. Olson, G. J., and F. E. Brinckman. Inorganic Materials Biotechnology: A New Industrial Measurement Challenge. J. Res. Natl. Bur. Standards, v. 91, No. 3, May-Jun. 1986, pp. 139-147.

13. Ehrlich, H. L. Recent Advances in Microbial Leaching of Ores. Miner. and Metall. Proc., May 1988, pp. 57-60.

14. Ehrlich, H. L. What Types of Microorganisms are Effective in Bioleaching, Bioaccumulation of Metals, Ore Beneficiation, and Desulfurization of Fossil Fuels? Biotechnology and Bioengineering Symp., No. 16, John Wiley and Sons, 1986, pp. 227-237.

15. Johnson, A. M., D. H. Carlson, S. T. Bagley, and D. L. Johnson. Investigations Related to In Situ Bioleaching of Michigan Chalcocite Ores. Min. Eng. (Littleton, CO), v. 40, No. 12, Dec. 1988, pp. 1119-1122.

16. Drever, J. I. The Geochemistry of Natural Waters. Prentice-Hall, 2nd ed., 1988, pp. 127-132.

17. Pohlman, S. L., and F. A. Olson A Kinetic Study of Acid Leaching of Chrysocolla Using a Weight Loss Technique. Ch. in Solution Mining Symposium Proceedings, 1974, pp. 446-460.

18. Potter, G. M., E. A. Nordhausen, J. B. Fletcher, J. L. Lake, J. V. Rouse, and F. Wojtasiak. Technological Investigation to Determine the Feasibility of In Situ Leaching Metallic Ores Other Than Copper and Uranium. (contract J0295032, Mountain States Res. and Dev., Inc.).

Volume 1, 1982, 140pp. (Available for consultation in the Library, BuMines, Minneapolis, MN.)

19. Roy, S. Manganese Deposits. Academic Press, 1981, 458 pp.

20. Burns, R. G., and V. M. Burns. Ch. in Marine Minerals, ed. by R. G. Burns. Mineralogy Society of America, 1979, pp 1-46.

21. Gay-Lussac and Welter. Ann. Chim. Phys., v.10, 1819, p. 312.

22. Meyer, J., and W. Schramm. Zeit. anorg. Chem., v. 132, 1923, p 226.

23. Dean, R. S., Leaver, E. S., and Joseph, T. L. Manganese; Its Occurrence, Milling, and Metallurgy, Part III. BuMines IC 6770, 1934, pp. 167-189.

24. Wyman, W. F., and S. F. Ravitz. Sulfur Dioxide Leaching Tests on Various Western Manganese Ores. BuMines RI 4077, 1947, 12 pp.

25. Bassett, H., and W. G. Parker. The Oxidation of Sulfurous Acid. J. Chem. Soc. London, 1951, pp. 1540-1560.

26. Higginson, W. C. E. and J. W. Marshall. Equivalence Changes in Oxidation-Reduction Reactions in Solution: Some Aspects of the Oxidation of Sulphurous Acid. J. Chem. Soc. (London), 1957, pp. 447-58.

27. Back, A. E., S. F. Ravitz, and K. E. Tame. Formation of Dithionate and Sulfate in the Oxidation of Sulfur Dioxide by Manganese Dioxide and Air. BuMines RI 4931, 1952, 14 pp.

28. Herring, A. P., and S. F. Ravitz. Rate of Dissolution of Manganese Dioxide in Sulfurous Acid. SME Transactions, v. 232, 1965, pp. 191-196.

29. Henn, J. J., R. C. Kirby, and L. D. Norman. Review of Major Proposed Processes for Recovering Manganese from United States Resources. (in three parts). 3. Sulfur Dioxide Processes. BuMines IC 8368, 1968, 36 pp.

30. Mansurkar, M. M., and S. K. Raman. Productivity of a Liquid Phase Batch Reactor for the Reaction between Sulfur Dioxide and Pyrolusite Ore. Indian J. of Tech., v. 13, March 1975, pp. 130-134.

31. Miller, J. D., and R. Wan. Reaction Kinetics for the Leaching of MnO_2 by Sulfur Dioxide. Hydromet., v. 10, 1983, pp. 219-242.

32. Canterford, J. H. Cobalt Extraction and Concentration from Manganese Wad by Leaching and Precipitation. Hydromet., v. 12, 1984, pp. 335-354.

33. Asai, S., H. Negi, and Y. Konishi. Reductive Dissolution of Manganese Dioxide in Aqueous Sulfur Dioxide Solutions. Can. J. Chem. Engr., v. 64, 1986, pp. 237-242.

34. Dixit, S. G. and P. R. Raisoni. Effect of Oxygen on the Leaching of Manganese Dioxide by Aqueous Sulfur Dioxide Solution. Indian J. Tech., v. 25, 1987, pp. 517-5199.

35. Raisoni, P. R., and S. G. Dixit. Leaching of Manganese Ore with Aqueous Sulfur Dioxide Solutions. Bull. Mater. Sci., v. 10, 1988, pp. 479-483.

36. Lee, J. H., J. Gilje, H. Zeitlin, and Q. Fernando. Low-temperature Interaction of Sulfur Dioxide with Pacific Ferromanganese Nodules. Environ. Sci. Tech., v. 12, 1978, pp. 1428-1431.

37. Warren, I. H., and E. A. Devuyst. Leaching of Iron and Manganese with Ammonium Carbamate. Transactions of SME, AIME, v. 252, 1972, pp. 388-391.

38. Malti, M. A., M. W. Rophael, and I. I. Bhayat. The Kinetics of Pyrophosphate Leaching of Partially Reduced Manganese Dioxides. Electrochim. Acta, v. 26, 1981, pp. 239-243.

39. Han, K. N., and D. W. Fuerstenau. Extraction Behavior of Metal Elements from Deep-Sea Manganese Nodules in Reducing Media. Marine Mining, v. 2, 1980, pp. 155-169.

40. Usatenko, Y. I., and A. S. Ryl'kova. Dissolution Kinetics of Manganese Oxide Ores in an Acetic Acid Solution of Potassium Iodide. J. Anal. Chem. U.S.S.R. (English version), v.38, 1983, pp. 66-70.

41. Dresler, W. Leaching of Manganese Dioxide in Nitrous Acid. Can. Metall. Quart., v. 23, 1984, pp. 271-279.

42. Dobos, G. Studies on the Kinetics of Ion-exchange Leaching of the Hungarian Rhodocrosite Ore of Urkut Origin. Reactive Polymers, v. 7, 1988, pp. 277-288.

43. U.S. Department of Interior. U.S. Bureau of Mines RESEARCH 88, 1988, p. 9.

44. Woods, T. L., and R. M. Garrels. Thermodynamic Values at Low Temperature for Natural Inorganic Materials. Oxford U. Press, 1987, 270 pp.

45. Cotton, F. A., and G. Wilkinson. Advanced Inorganic Chemistry. Wiley-Interscience, 5th ed., 1980, p. 741.

46. Hoffman, M. R. Thermodynamic, Kinetic, and Extrathermodynamic Considerations in the Development of Equilibrium Models for Aquatic Systems. Environ. Sci. Tech., v. 15, 1981, pp. 345-53.

47. Stumm, W., and J. J. Morgan. Aquatic Chemistry. Wiley-Interscience, 1981, 780 pp.

48. Morgan, J. J. Principles of Metal Speciation and Transport, Workshop: Metal Speciation and Transport in Groundwaters, May 24-26, 1989, Jekyll Island, GA.

49. Pandow, J. E., and J. J. Morgan. Kinetics for the Aquatic Environment. Part 1. Environ. Sci. Tech., v. 15, 1981, pp. 1155-64.

50. Pandow, J. E., and J. J. Morgan. Kinetics for the Aquatic Environment. Part 2. Environ. Sci. Tech., v. 15, 1981, pp. 1306-13.

51. Lasaga, A. C. Ch. in Kinetics of Geochemical Processes. Reviews in Mineralogy, ed. by A. C. Lasaga and R. J. Kirkpatrick, Mineral. Soc. Am., v. 8, 1981, pp. 1-68.

52. Wilkinson, F. Chemical Kinetics and Reaction Mechanisms. Van Nostrand, 1980, 335 pp.

53. Gilliom, R. D. Introduction to Physical Organic Chemistry. Addison-Wesley, 1970, pp. 120-26.

54. Levine, I. N. Physical Chemistry. McGraw-Hill, 3rd. ed., 1988, pp. 834-53.

55. Habashi, F. Principles of Extractive Metallurgy. Gordon and Breach, 1969, v. 1, 413 pp.

56. Berner, R. A. Rate Control of Mineral Dissolution under Earth Surface Conditions. Am. J. Sci., v. 278, 1978, pp. 1235-52.

57. Blum, A. E., and A. C. Lasaga. Ch. in Aquatic Surface Chemistry, ed. by W. Stumm, Wiley-Interscience, 1988, pp. 255-92.

58. Schott, J., S. Brantley, D. Crerar, C. Guy, M. Borcsik, and C. Willaime. Dissolution Kinetics of Strained Calcite. Geochim. Cosmochim. Acta, v. 53, 1989, pp. 373-82.

59. Stumm, W., and G. Furrer. Ch. in Aquatic Surface Chemistry, ed. by W. Stumm, Wiley-Interscience, 1987, pp. 197-219.

60. Stone, A. T., and J. J. Morgan. Ch. in Aquatic Surface Chemistry, ed. by W. Stumm, Wiley-Interscience, 1987, pp. 221-254.

61. Gileadi, E., E. Kironwa-Eisner, and J. Penciner. Interfacial Electrochemistry. Addison-Wesley, 1975, pp. 1-15.

62. Schindler, P. W., and W. Stumm. Ch. in Aquatic Surface Chemistry, ed. by W. Stumm, Wiley-Interscience, 1988, pp. 83-110.

63. Furrer, G., and W. Stumm. The Coordination Chemistry of Weathering: I. Dissolution Kinetics of δ-Al_2O_3 and BeO. Geochim. Cosmochim. Acta, v. 50, 1986, pp. 1847-60.

64. Bettina Zinder, G. Furrer, and W. Stumm. The Coordination Chemistry of Weathering: II. Dissolution of Fe (III) oxides. Geochim. Cosmochim. Acta, v. 50, 1986, pp. 1861-69.

65. Stone, A. T., and J. J. Morgan. Reduction and Dissolution of Manganese (III) and Manganese (IV) Oxides by Organics. 1. Reaction with Hydroquinone. Environ. Sci. Tech., v. 18, 1984, pp 450-6.

66. Stone, A. T., and J. J. Morgan. Reduction and Dissolution of Manganese (III) and Manganese (IV) Oxides by Organics. 2. Survey of the Reactivity of Organics. Environ. Sci. Tech., v. 18, 1984, pp 817-24.

67. Taube, H. Electron-transfer between Metal Complexes: Retrospective. Science, v. 226, 1984, pp. 1028-1036.

68. Laha, S. and R. G. Luthy. Oxidation of aniline and other primary aromatic amines by manganese dioxide. Enviro. Sci. Tech., v. 24, 1990, pp. 363-373.

69. Wieland, E., B. Wehrli, and W. Stumm. The coordination chemistry of weathering: III A generalization on the dissolution rates of minerals. Geochim. Cosmochim. Acta, v. 52, 1988, pp. 1969-1981.

70. Stumm, W., and R. Wollast. Coordination Chemistry of Weathering: Kinetics of the Surface-Controlled Dissolution of Oxide Minerals. Rev. Geophy., v. 28, 1990, pp. 53-69.

71. Zoltai, T. and J. H. Stout. Symmetry and Atomic Bonding. Ch. in Mineralogy, Concepts and Principles, MacMillian, 1984, pp. 69-107.

72. Jolly, W. L. Kinetics and mechanisms of reactions of transition-metal complexes. Ch. in Modern Inorganic Chemistry, McGraw-Hill, 1984, pp. 447-469.

73. Taube, H. Chem. Rev., v. 50, 1952, p. 69.

74. Basolo, F. and R. G. Pearson. Mechanisms of Inorganic Reactions. 2nd ed., 1967, Wiley, pp. 145-158.

75. Luther, G. W. Pyrite oxidation and reduction: Molecular orbital theory considerations. Geochim. Cosmochim. Acta, v. 51, 1987, pp. 3193-3199.

76. Luther, G. W. The frontier-molecular-orbital theory approach in geochemical processes. Ch. in Aquatic Chemical Kinetics, ed. by W. Stumm, 1990, Wiley, pp 173-198.

77. Burdige, D. J. and K. H. Nealson. Chemical and microbiological studies of sulfide-mediated manganese reduction, Geomicrobio., v. 4, 1986, pp. 361-387.

78. Correlation Analysis in Chemistry, Recent Advances, ed. by N. B. Chapman and J. Shorter, Plenum Press, 1978, 575 pp.

79. Purser, G. H. The significance of the bond angle in sulfur dioxide. J. Chem. Ed., v. 66, 1989, pp. 710-713.

80. Schenk, W. A. Sulfur oxides as ligands in coordinate compounds. Angew. Chem. Int. Ed. Engl., v. 26, 1987, pp. 98-109.

81. Gimarc, B. M. Molecular Structure and Bonding. The Qualitative Molecular Orbital Approach. Academic Press, 1979, pp. 153-169.

82. CRC Handbook of Chemistry and Physics, ed. by D. R. Lide, CRC Press, 71st ed., 1990, 2240 pp.

TABLE 1. - Types of mineral surface chemical reactions

Physical Adsorption
Chemisorption (Surface Complexation)
Dissolution
Precipitation
Oxidation-Reduction
Biochemical

TABLE 2. - Locations of significant U.S. manganese ore deposits

Artillery Peak, Arizona (oxides)
Batesville, Arkansas (manganiferous limestone)
San Juan Mountains, Colorado (silicates)
Chamberlain, South Dakota (manganese nodules)
Aroostook County, Maine (silicates and carbonates)
Cuyuna Range, Minnesota (oxides and carbonates)

TABLE 3. - Mn ore sample characteristics[7]

Sample	District	County and State	Mn[1] Form	Mn minerals	Principal gangue minerals	Origin
AZ-1..	Harshaw.....	Santa Cruz, AZ..	Ox.....	Psilomelane, pyrolusite, braunite.	Anglesite, quartzite, felsite, rhyolite, galena.	4
AZ-2..	..do.....	..do.....	..do...	Psilomelane, pyrolusite.	Quartzite, anglesite, felsite, rhyolite, galena.	4
AZ-3..	Tombstone.....	Cochise, AZ.....	..do...	..do.....	Quartz, calcite, dolomite.	4
AZ-4..	..do.....	..do.....	..do...	..do.....	..do.....	4
AZ-5..	Artillery Peak....	Mohave, AZ.....	..do...	Wad, pyrolusite, psilomelane	Quartz, albite, calcite, clay.	3
AR-1..	Batesville.....	Independence, AR	..do...	Hausmannite, braunite, wad, psilomelane, pyrolusite.	Calcite, clay, hematite, chert.	4
AR-2..	..do.....	..do.....	..do...	..do.....	..do.....	4
CA-1..	Paymaster.....	Imperial, CA....	..do...	Manganite, pyrolusite, psilomelane.	Calcite, barite, chalcedony.	4
CO-1..	Leadville.....	Lake, CO.....	..do...	Psilomelane, pyrolusite, manganosiderite.	Quartz, calcite, hematite, goethite.	4
CO-2..	Silvercliff.....	Custer, CO.....	Ox.....	Cryptomelane.	Quartz, hematite.	4
CO-3..	San Juan.....	San Juan, CO....	Sil....	Rhodonite[2]	Quartz, chalcedony, galena, sphalerite, pyrite.	4
ME-1..	Aroostook.....	Aroostook, ME...	Carb-sil	Braunite, bementite, rhodochrosite.	Hematite, quartz, pyrite, calcite.	5
ME-2..	..do.....	..do.....	..do...	Rhodonite, braunite, bementite, rhodochrosite.	..do.....	5
MN-1..	Cuyuna.....	Crow Wing, MN...	Ox-carb	Rhodochrosite, manganite, pyrolusite.	Goethite, siderite, quartz, groutite.	3
MN-2..	..do.....	..do.....	Ox.....	Stilpnomelane, pyrolusite.	Hematite, quartz.	3
MN-3..	..do.....	..do.....	..do...	Manganite, pyrolusite, stilpnomelane.	Hematite, quartz, talc.	3
MN-4..	..do.....	..do.....	..do...			
MN-5..	..do.....	..do.....	..do...	..do.....	..do.....	3
NV-1..	Pioche.....	Lincoln, NV.....	..do...	Pyrolusite, stilpnomelane.	..do.....	3
NV-2..	Three Kids.....	Clark, NV.....	..do...	Manganite, braunite.	Goethite, quartz, calcite.	4
NV-3..	Virgin River.....	..do.....	..do...	Wad, psilomelane, manganite.	Quartz, clay, mica, hematite, calcite	3
NV-4..	Boulder City.....	..do.....	..do...	Wad, psilomelane.	..do.....	3
NV-5..	Pioche.....	Lincoln, NV.....	..do...	..do.....	Selenite, limonite, quartz, calcite.	3
NV-6..	..do.....	..do.....	..do...	Pyrolusite.	Calcite, quartz.	4
SD-1..	Chamberlain.....	Lyman, SD.....	Carb...	..do.....	Siderite, galena, dolomite, quartz.	4
				Manganocalcite, pyrolusite, manganite.	Siderite, calcite, dolomite, quartz, clay.	6

[1] Ox oxide, Sil silicate, Carb carbonate.
[2] May be the pyroxmanganite variety.
[3] Sedimentary.
[4] Hydrothermal vein
[5] Submarine volcanic, sedimentary
[6] Fossil sea nodules, sedimentary.
[7] Source: Reference 8.

TABLE 4. - Composition and structure of key U.S. manganese minerals

Mineral	Composition	Structure	Oxidation of Mn	Coordination Number
pyrolusite	β-MnO_2	tetragonal	+4	6
romanechite (psilomelane)	$Ba(OH)_4Mn^{2+}Mn^{4+}{}_8O_{16}$	monoclinic	+4 +2	6 6
hausmannite	$Mn^{2+}Mn^{3+}{}_2O_4$	tetragonal	+3 +2	6 4
manganite	γ-MnOOH	monoclinic	+3	6
braunite	$(Mn^{3+}{}_2O_3)_3Mn^{2+}SiO_3$	tetragonal	+3 +2	6 6
rhodochrosite	$MnCO_3$	trigonal (rhombohedral)	+2	6
rhodonite	$MnSiO_3$	triclinic	+2	6

TABLE 5. - Predominant manganese minerals on the Cuyuna Range, Minnesota

Mineral	Composition	Structure	Oxidation of Mn	Coordination Number
pyrolusite	β-MnO_2	tetragonal	+4	6
manganite	γ-MnOOH	monoclinic	+3	6
romanechite (psilomelane)	$Ba(OH)_4Mn^{2+}Mn^{4+}{}_8O_{16}$	monoclinic	+4 +2	6 6
rhodochrosite	$MnCO_3$	trigonal (rhombohedral)	+2	6

TABLE 6. - Formation of $S_2O_6^=$ vs. O_2 concentration and temperature[1]

Oxygenated Solution	Temperature (°C)	$S_2O_6^=$ Yield (%)[2]
No	25	54
No	75	22
No	95	7
Yes	25	21
Yes	75	8
Yes	95	trace

[1] Source: Reference 35.

[2] $S_2O_6^=$ yield $= \frac{[S_2O_6^=]}{[S_2O_6^=] + [SO_4^=]} \times 100\%$

TABLE 7. - Batch leaching efficiencies for U.S. manganese ores[1]

Manganese Ore Mineralogy	No. of Samples[2]	Mn leached (%) Ave.	Mn leached (%) Range	Ca leached (%) Ave.	Ca leached (%) Range	Fe leached (%) Ave.	Fe leached (%) Range
pyrolusite,romanechite	6	95 ± 3	91-98	56 ± 25	25-81	14 ± 7[3]	1-25
hausmannite,braunite	2	79 ± 6	76-81	70 ± 20	56-84	4 ± 2	2-5
rhodochrosite	3	67 ± 11	55-76	64 ± 15	48-78	9 ± 1[3]	1-9
manganite	2	59 ± 7	54-64	34, 92[4]	34-92	5 ± 2	3-6
rhodonite	2	0	0	23, 75[4]	23-75	1, 23[4]	1-23

[1] Batch leach of -0.841 mm particles with 6.4 wt % SO_2 at pH 1.1 for 30 minutes at ambient temperature and pressure. Source: Pahlman and Khalafalla (8).

[2] Each sample represents a different ore body, generally from a different state, which contains the predominant manganese minerals listed.

[3] One sample had a 1% Fe leaching efficiency which was not used in the average.

[4] Due to the large difference between the two numbers, no average was calculated.

TABLE 8. - Thermodynamic evaluation of Mn leaching in U.S. manganese ores[1]

Mineral	Probable Overall Leaching Reaction[1]	ΔG° (kJ/mole Mn^{2+})
pyrolusite	$Mn^{4+}O_2(s) + SO_2 = Mn^{2+} + SO_4^{=}$	-209
	$Mn^{4+}O_2(s) + 2SO_2 = Mn^{2+} + S_2O_6^{=}$	-131
romanechite	most Mn sites similar to pyrolusite	-209 or -131
hausmannite	$1/3Mn^{2+}Mn^{3+}{}_2O_4(s) + 1/3SO_2 + 4/3H^{+} = Mn^{2+} + 1/3SO_4^{=} + 2/3H_2O$	-110
braunite	Mn_2O_3 sites: $1/2Mn^{3+}{}_2O_3(s) + 1/2SO_2 + H^{+} = Mn^{2+} + 1/2SO_4^{=} + 1/2H_2Os$	-131
	$Mn^{2+}SiO_3$ site: $Mn^{2+}SiO_3(s) + 2H^{+} = Mn^{2+} + SiO_2(amorp) + H_2O$	-76
rhodochrosite	$Mn^{2+}CO_3 + 2H^{+} = Mn^{2+} + H_2O + CO_2(gas)$	44
manganite	$Mn^{3+}OOH(s) + H^{+} + 1/2SO_2 = Mn^{2+} + 1/2SO_4^{=} + H_2O$	-132
rhodonite	$Mn^{2+}SiO_3(s) + 2H^{+} = Mn^{2+} + SiO_2(amorphous) + H_2O$	-76

[1] The oxidation state of the Mn centers for each mineral site is given to emphasize the oxidation state changes that occur during dissolution at pH 1.1.

TABLE 9. - Thermodynamic evaluation of gangue[1] leaching in U.S. manganese ores

Mineral	Probable Overall Leaching Reaction	ΔG^o (kJ/mole)
quartz	$SiO_2(q) + 2H_2O = H_4SiO_4(amorphous)$	+23
calcite	$CaCO_3(s) + 2H^+ = Ca^{2+} + H_2O + CO_2(gas)$	-56
hematite	$Fe_2O_3(s) + 6H^+ = 2Fe^{3+} + 3H_2O$	-5
geothite	$FeO(OH)(s) + 3H^+ = Fe^{3+} + 2H_2O$	-2
siderite	$FeCO_3(s) + H^+ = Fe^{3+} + HCO_3^-$	+75

[1] The gangue minerals listed were those most frequently found in the manganese ores. The reactions are for solution pH values < 1. Source: Reference 8.

TABLE 10. - Surface coordination model for mineral leaching[1]

1. Diffusion of solution-phase reactant molecules (or atoms) to the mineral surface.
2. Rapid adsorption of reactant molecules at mineral surface sites with highest energy, polarizing and weakening metal-oxygen bonds.
3. Slow detachment of metal species from the mineral surface.
4. Diffusion of detached metal species into the bulk solution.

[1] Source: Reference 56.

TABLE 11. - Reductive dissolution mechanism for the surface coordination model[1]

1. Diffusion of solution-phase reactant molecules (or atoms) to the mineral surface.
2. Rapid adsorption of reactant molecules at mineral surface sites with highest energy, forming inner-sphere or outer-sphere precursor complexes capable of electron transfer.
3. Electron transfer to create a metal center of lower oxidation state, expanding the metal center size and weakening metal-oxygen bonds.
4. Detachment of the oxidized reductant.
5. Detachment of reduced metal species from the mineral surface.
6. Diffusion of detached metal species into the bulk solution.

[1]Source: Reference 57.

TABLE 12. - Ionic radius ratios (r_+/r_-) for common mineral coordinations[1]

Minimum r_+/r_-	Coordination No.	Spatial Symmetry	Example
0	2	linear	cuprite (oxide)
0.155	3	triangular planar	carbonates, nitrates
0.225	4	tetrahedral	silicates
0.414	4	square planar	cooperite (sulfide)
0.414	5	tetrahedral pyramid	millerite (sulfide)
0.414	6	octahedral	halite
0.529	6	trigonal prism	molybdenite (sulfide)
0.625	8	square antiprism	scheelite (tungstate)
0.732	8	cube	fluorite
1.00	12	cuboctahedron	metals, alloys
1.00	12	disheptahedron	metals, alloys

[1]Source: Reference 71, p. 112.

TABLE 13. - Symmetry and coordination for common atomic orbital hybridizations

Orbital Hybridization	Resulting Spatial Symmetry	Coordination No.
sp	linear	2
sp^2	planar triangular	3
sp^3, sd^3	tetrahedral	4
d^2sp^3	octahedral	6
dsp^2	square planar	4
dsp^3	trigonal bipyramidal	6
dsp^3	square pyramidal	5

TABLE 14. - Ionic radius ratio for Mn-O ionic bonding

Cation	r_+/r_-
Mn^{4+}	0.386
Mn^{3+}	0.461
Mn^{2+}	0.593
Minimum for Octahedral	0.414

TABLE 15. - General rules for substitution reactivity of metal complexes in solution[1]

1. For a given central metal charge, the smaller the metal, the more inert (i.e. slower) its complexes are to substitution. This is because a smaller central metal holds its anionic ligands more tightly.

2. For a given central metal size, the higher the charge, the more inert its complexes are to substitution. This is again because a central metal with more formal charge holds its anionic ligands more tightly.

3. Reactivity of transition-metal complexes in octahedral symmetry is correlated to the 3d electron configuration of the metal ion as follows:

   Labile: d^0, d^1, d^2, d^4 (high spin), d^5 (high spin), d^6 (high spin), d^7, d^8, d^9, d^{10}

   Inert: d^3, d^4 (low spin), d^5 (low spin), d^6 (low spin)

Rule 3, first advanced by Taube (73), is based on the assertion that a complex with (1) one or more e_g^* antibonding electrons or (2) fewer than three d electrons is labile. Other configurations are relatively inert. Experimental evidence has largely supported this rule.[2]

[1] Source: Reference 72.

[2] Source: Reference 72, Table 19.1, p. 449.

List of Figure Captions

Preceding page blank

Figure 15. Qualitative MOT energy diagram for SO_2. The x-axis is perpendicular to the page. "*" denotes antibonding and "N" denotes non-bonding orbitals. Adapted from 81, p. 158

Figure 16. MOT treatment of 2-electron reduction of Mn^{4+} oxides by SO_2

Figure 17. MOT treatment of 1-electron reduction of Mn^{3+} oxides by SO_2

Figure 18. Mechanism of reductive dissolution of Mn oxides by SO_2

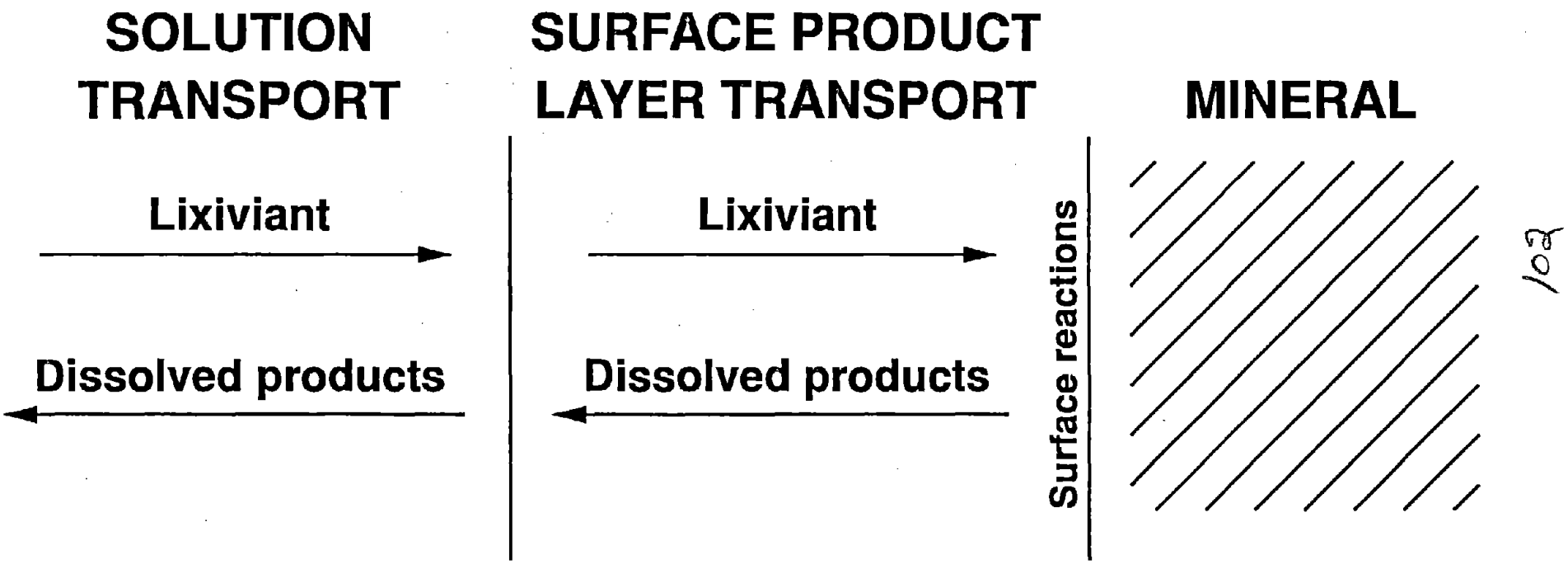
SOLUTION TRANSPORT
SURFACE PRODUCT LAYER TRANSPORT
MINERAL
Lixiviant
Lixiviant
Surface reactions
Dissolved products
Dissolved products
102

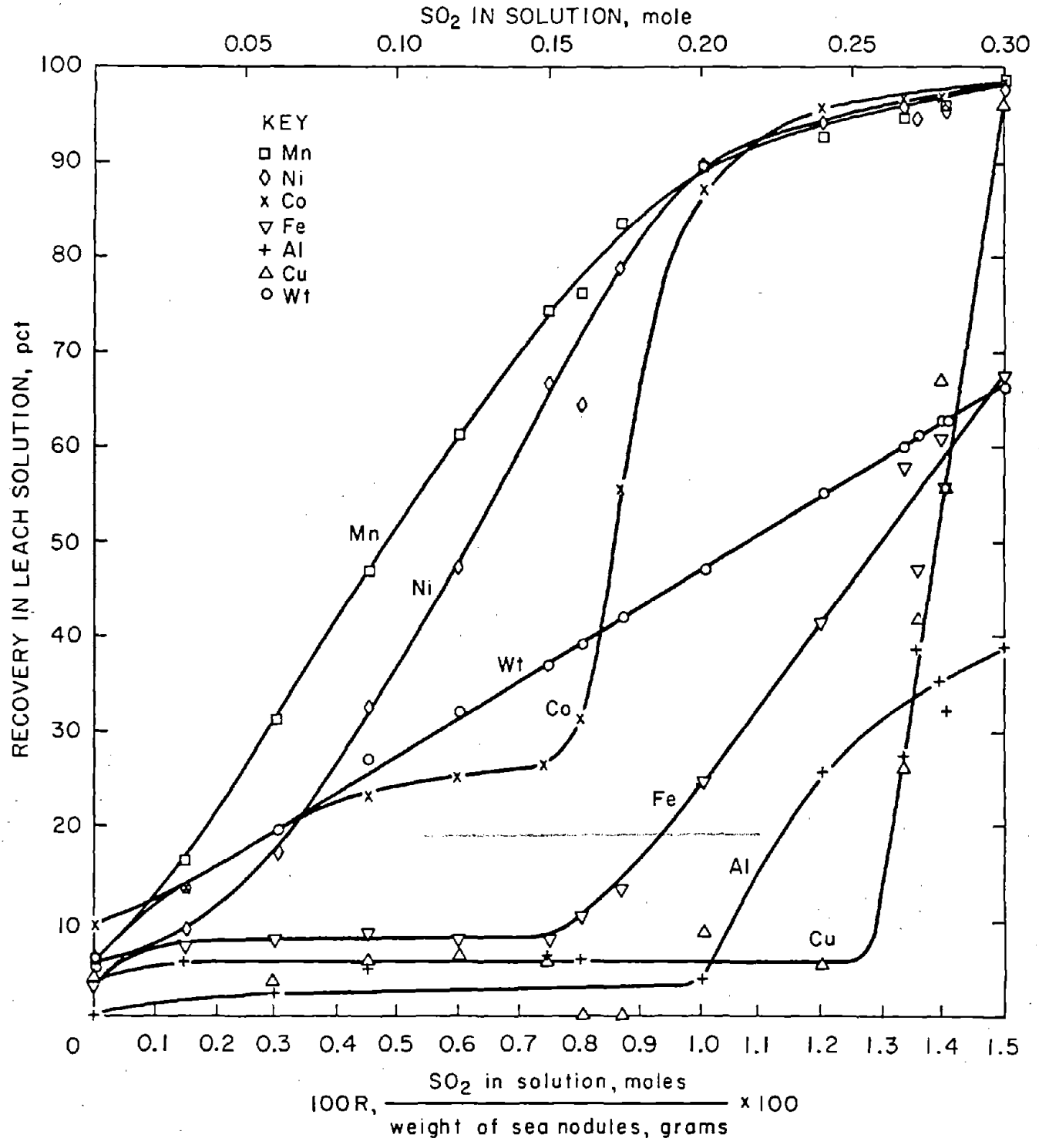
SO2 IN SOLUTION, mole
0.05
0.10
0.15
0.20
0.25
0.30
KEY
Mn
Ni
Co
Fe
Al
Cu
Wt
RECOVERY IN LEACH SOLUTION, pct
100
90
80
70
60
50
40
30
20
10
0
Mn
Ni
Wt
Co
Fe
Al
Cu
0.1
0.2
0.3
0.4
0.5
0.6
0.7
0.8
0.9
1.0
1.1
1.2
1.3
1.4
1.5
SO2 in solution, moles
100R, ——————————— x 100
weight of sea nodules, grams

GEOCHEMICAL CHARACTERIZATION

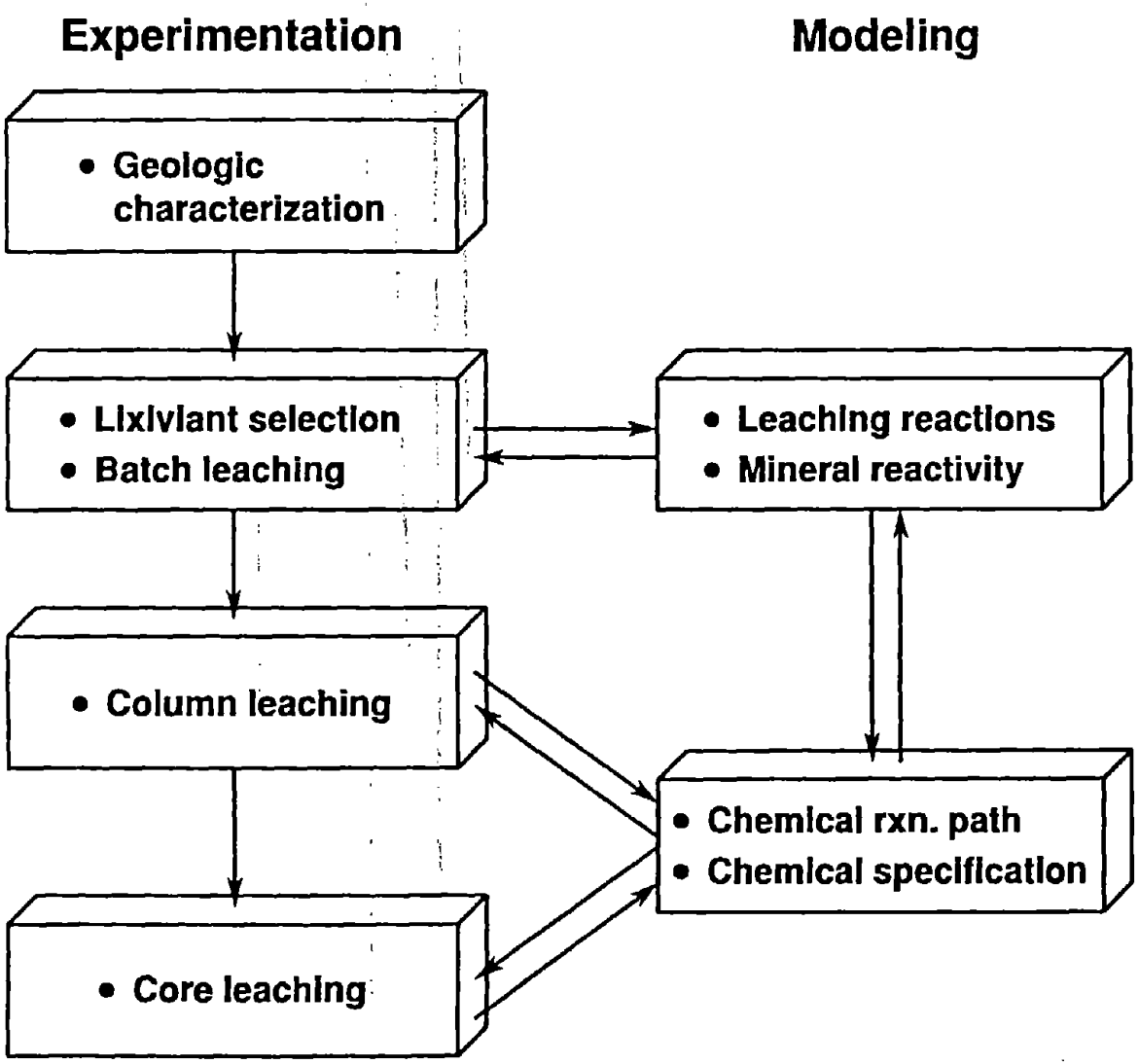

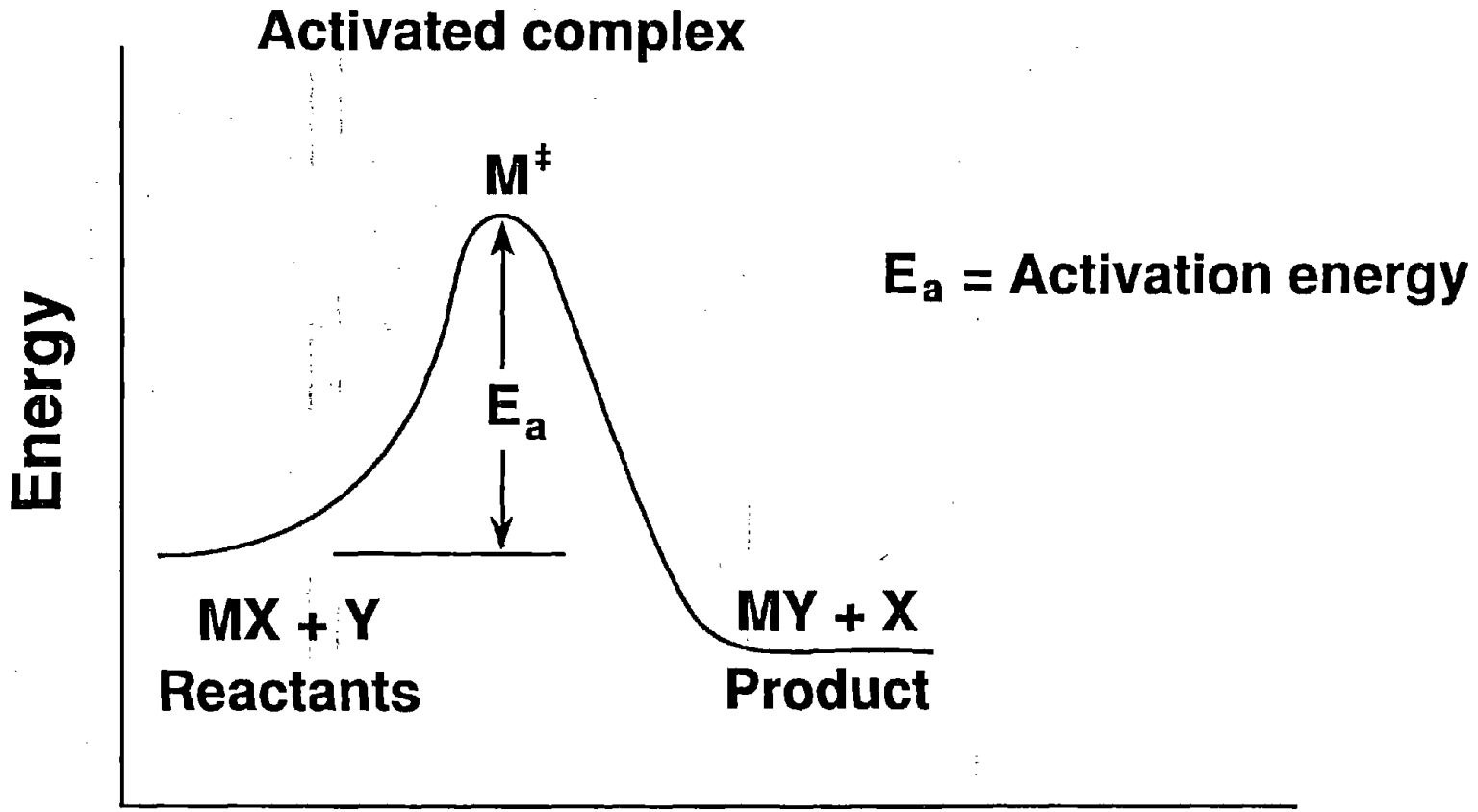
Activated complex
M‡
Energy
Ea
MX + Y
Reactants
MY + X
Product
Ea = Activation energy

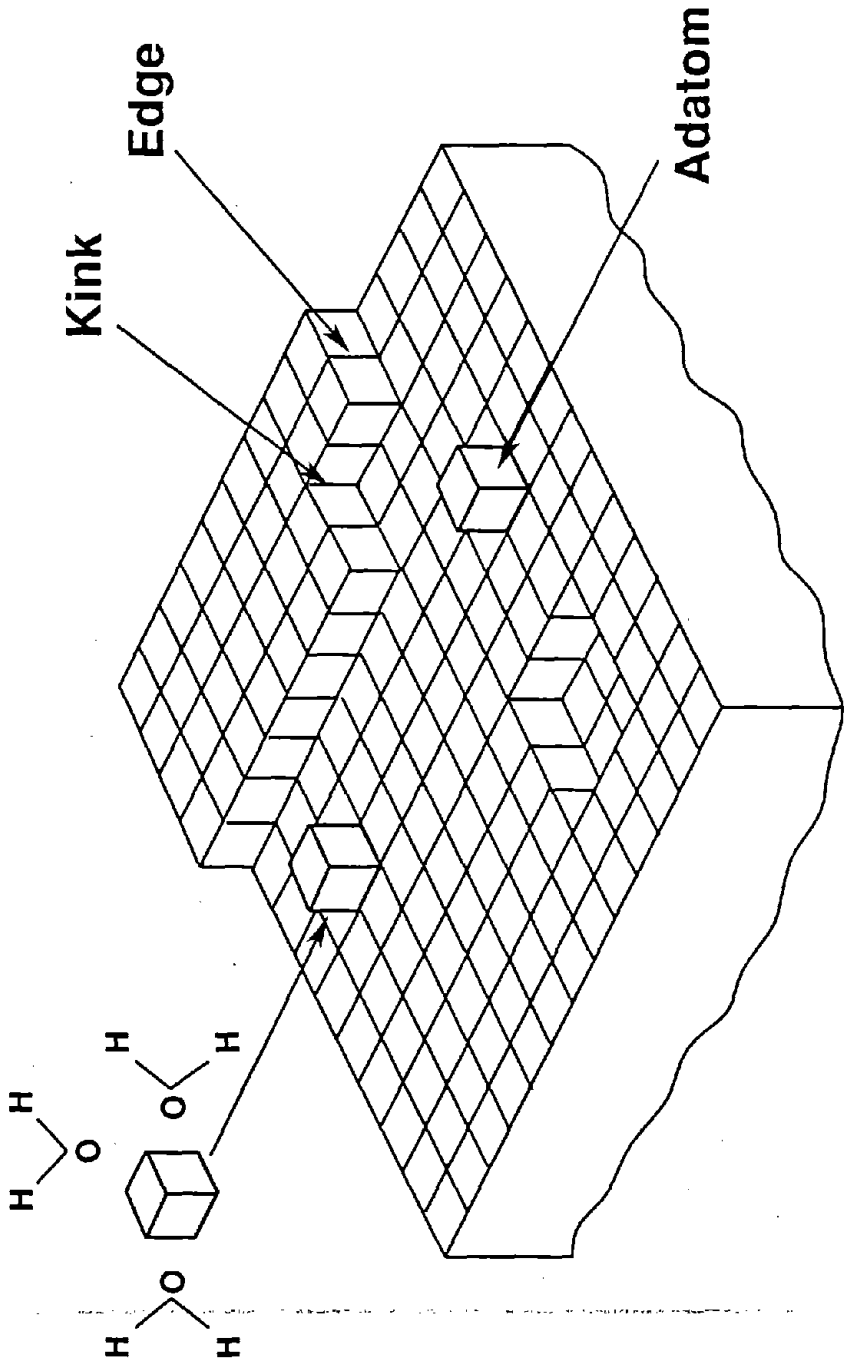
Edge
Kink
Adatom
H
O
H
H
O
H
O
H
H

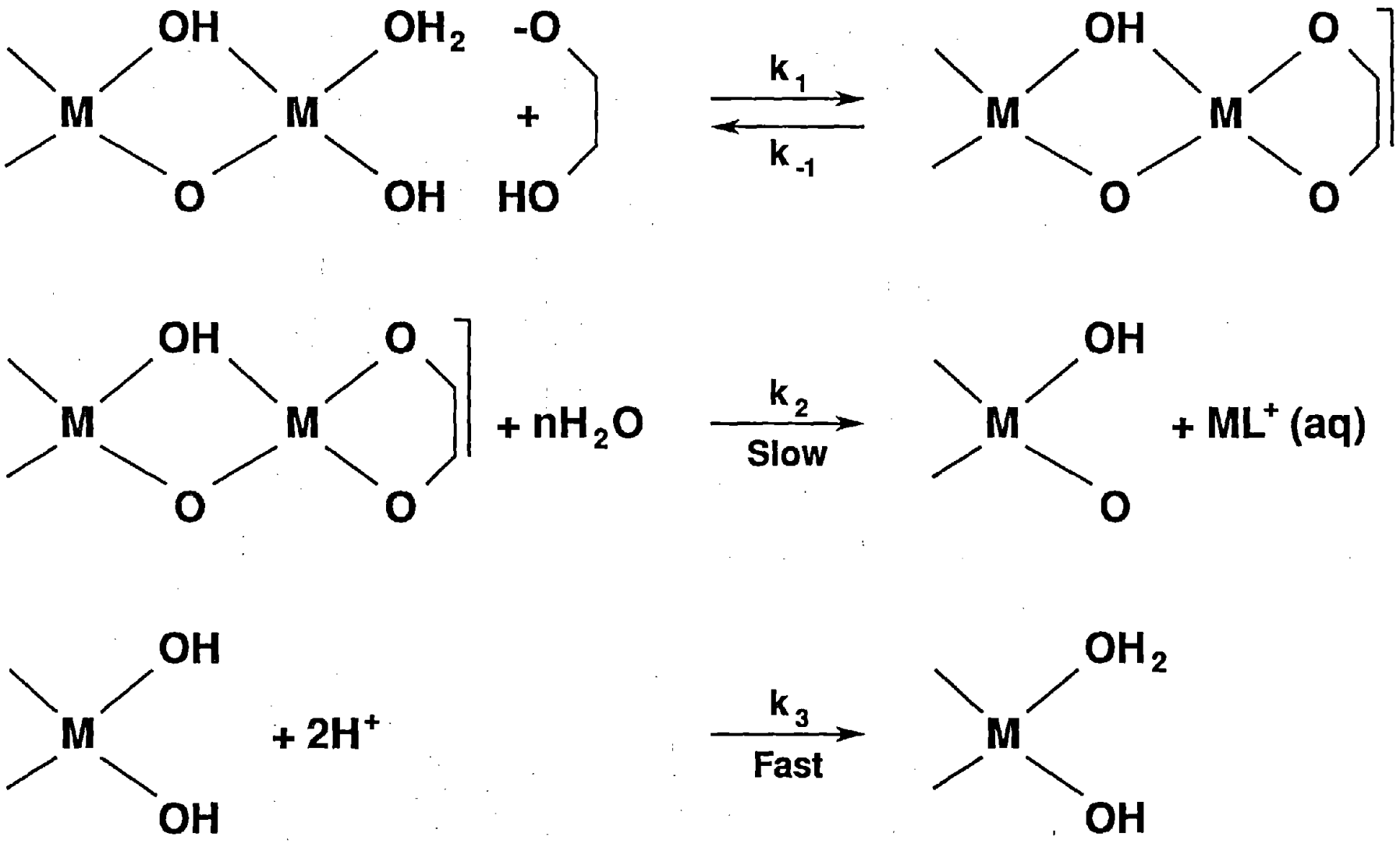
OH
OH2
-O
M
M
+
O
OH
HO
k1
k-1
OH
O
M
M
O
O
OH
O
M
M
+ nH2O
O
O
k2
Slow
OH
M
+ ML+ (aq)
O
OH
M
+ 2H+
OH
k3
Fast
OH2
M
OH

Aliphatic acids

$k_{oxalate}$ > $k_{malonate}$ > $k_{succinate}$

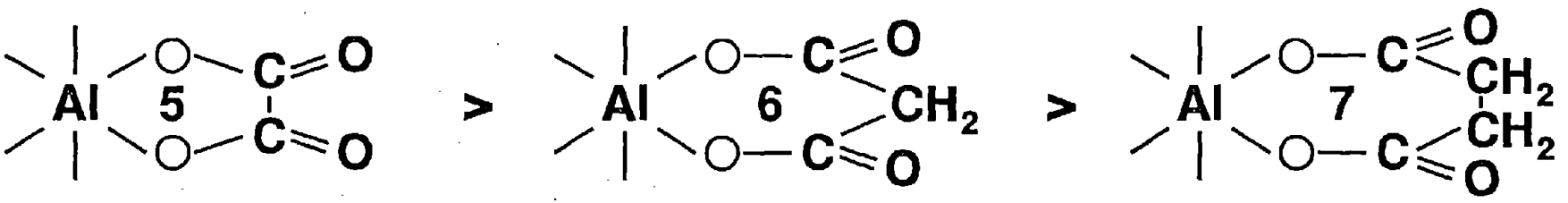

Aromatic acids

$k_{salicylate}$ > $k_{phthalate}$ >> $k_{benzoate}$

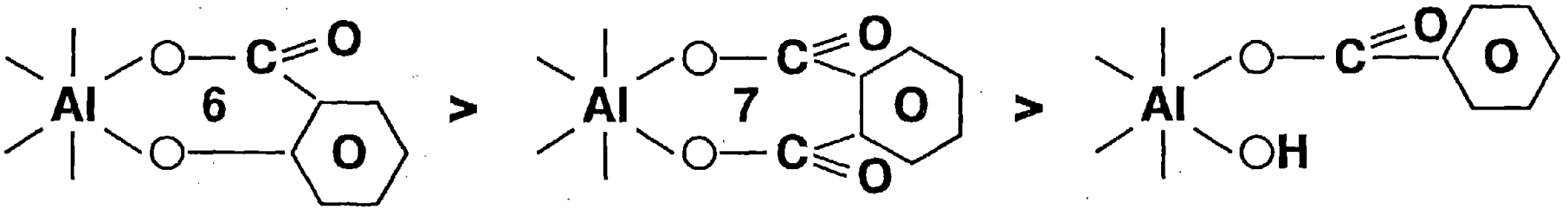

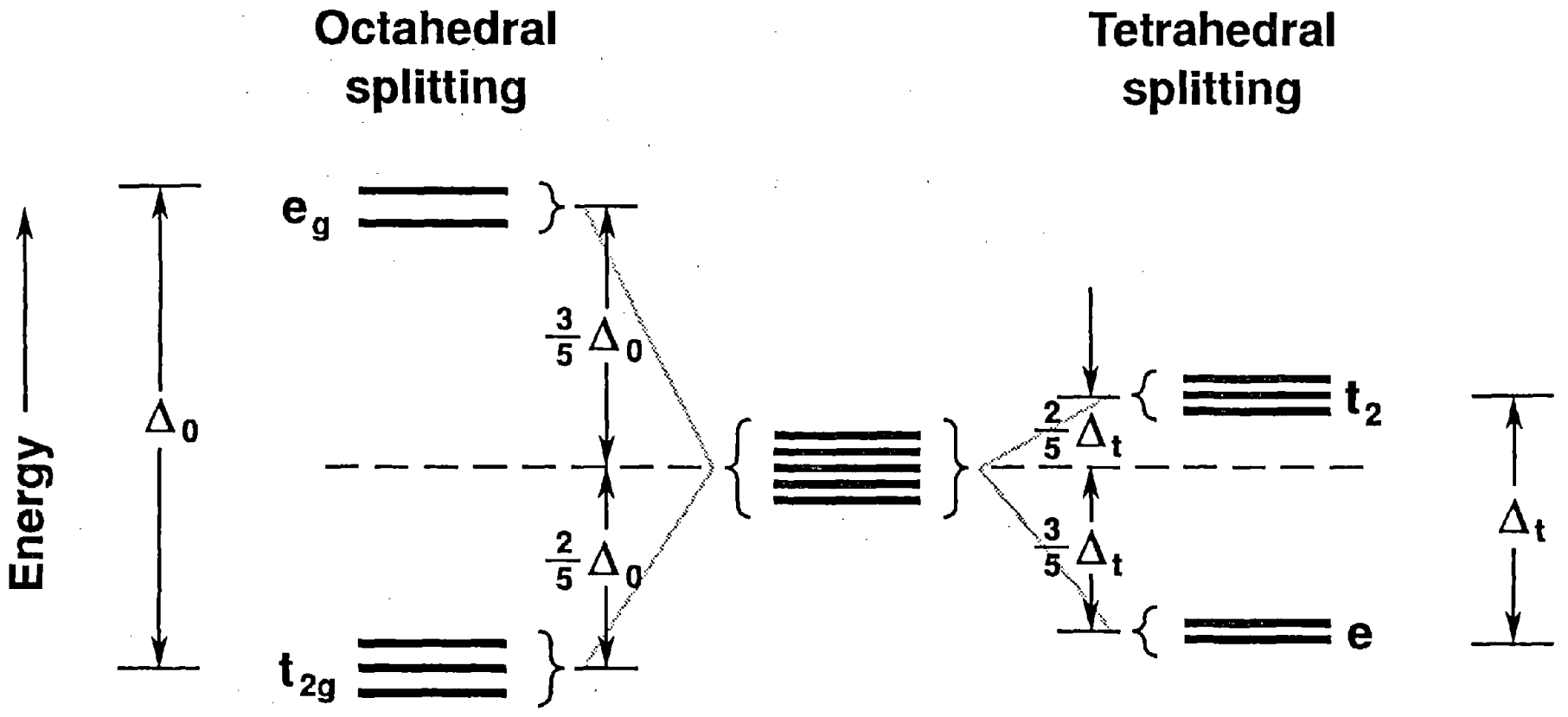
Octahedral splitting
Tetrahedral splitting
Energy
Δ_0
e_g
t_{2g}
$\frac{3}{5}\Delta_0$
$\frac{2}{5}\Delta_0$
t_2
e
$\frac{2}{5}\Delta_t$
$\frac{3}{5}\Delta_t$
Δ_t

Sigma (σ) molecular orbital

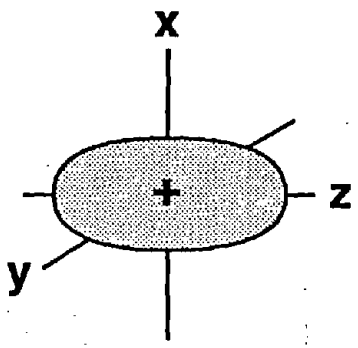

Pi (π) molecular orbitals

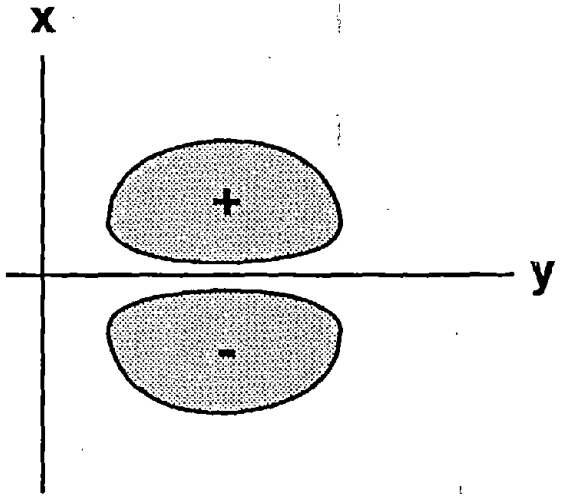

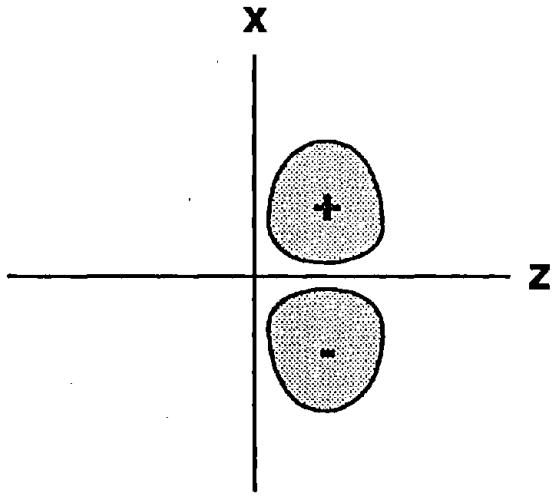

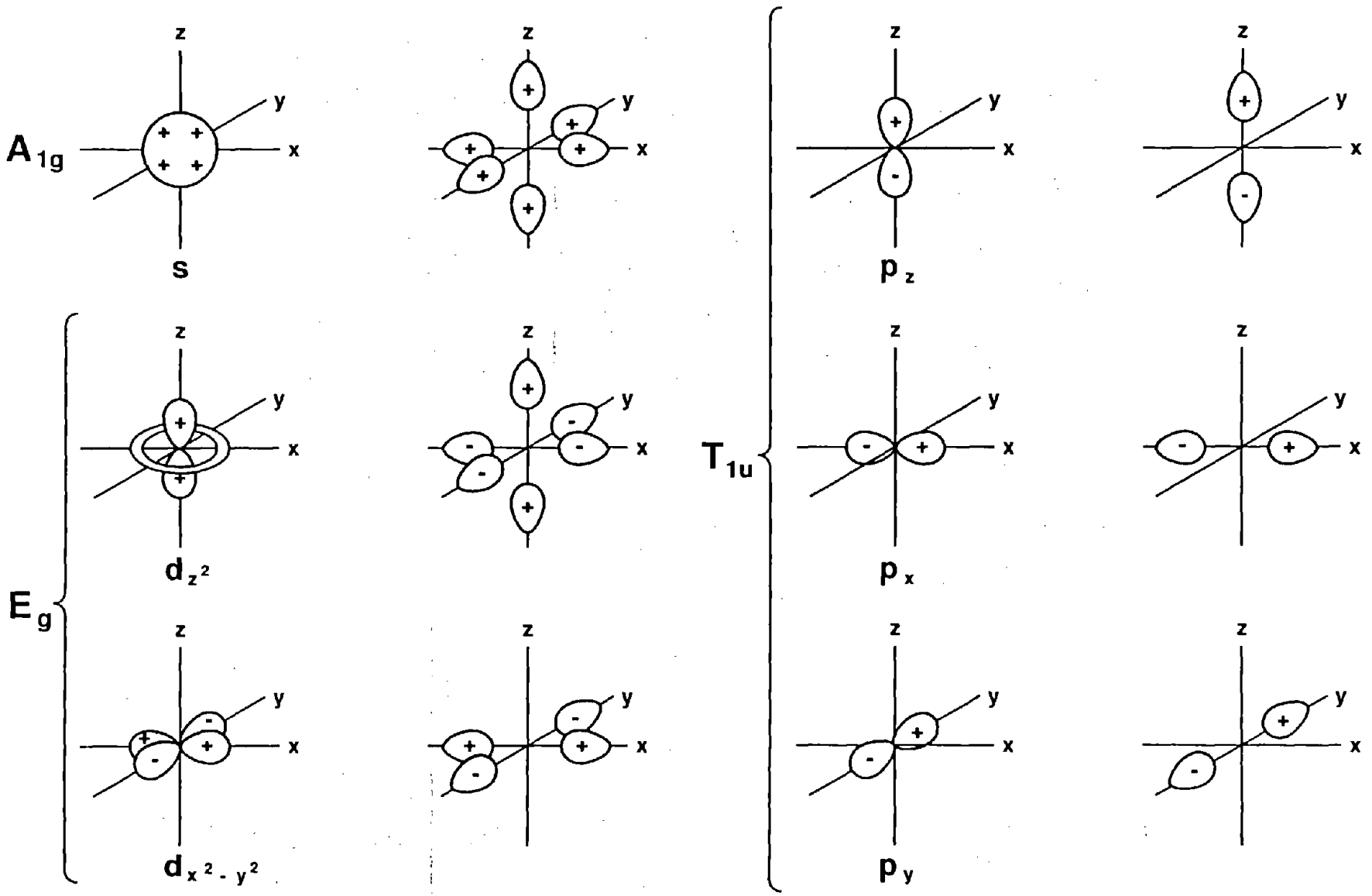
A1g
s
Eg
dz²
dx²-y²
T1u
pz
px
py
z
y
x

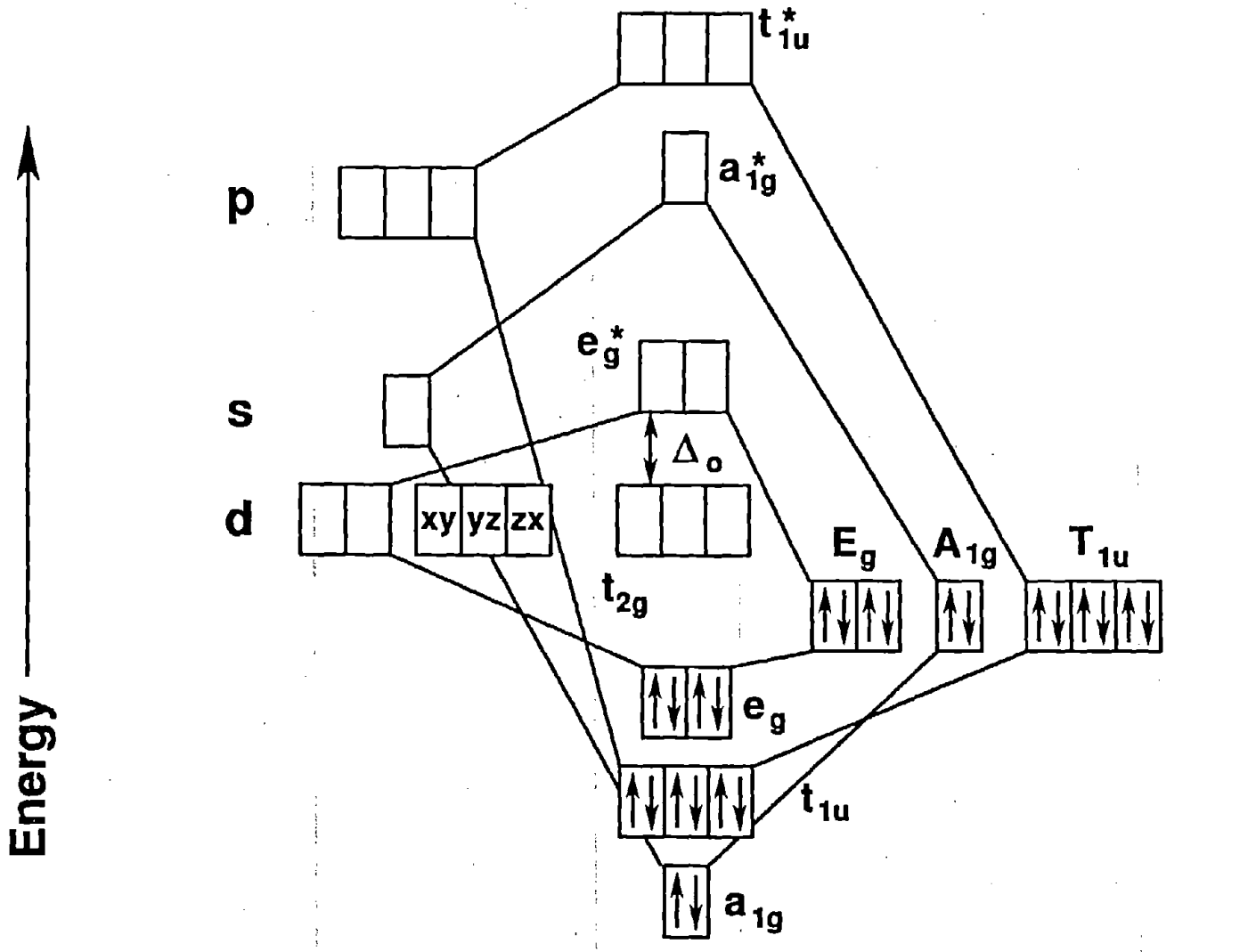
Energy
p
s
d
xy yz zx
t^*_{1u}
a^*_{1g}
e^*_g
Δ_o
t_{2g}
E_g
A_{1g}
T_{1u}
e_g
t_{1u}
a_{1g}
Metal orbitals
Molecular orbitals
Ligand group orbitals

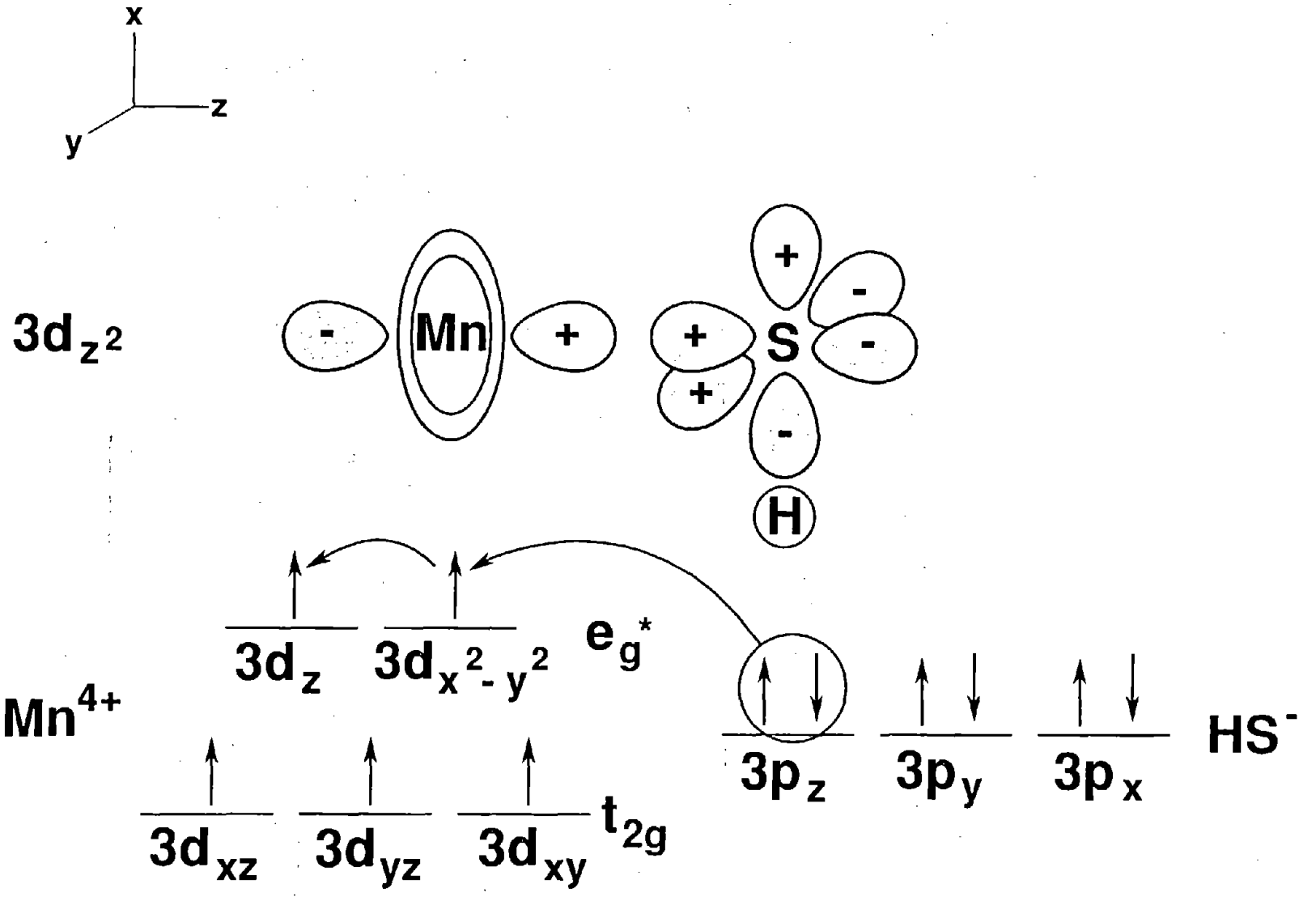
x
z
y
3d$_{z^2}$
Mn
S
H
3d$_z$
3d$_{x^2-y^2}$
e$_g$*
Mn^{4+}
3d$_{xz}$
3d$_{yz}$
3d$_{xy}$
t$_{2g}$
3p$_z$
3p$_y$
3p$_x$
HS$^-$

Resonance π bonding

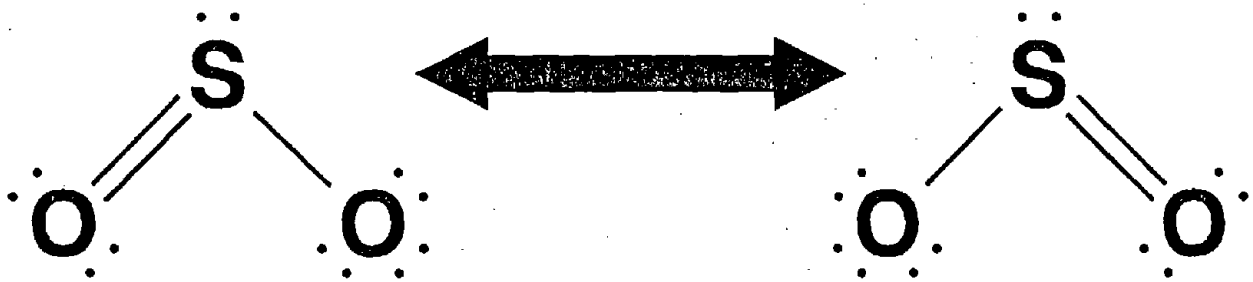

Stable π double bonding

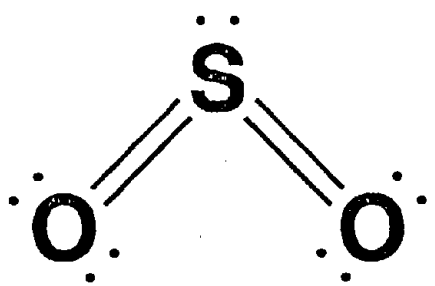

Pyramidal

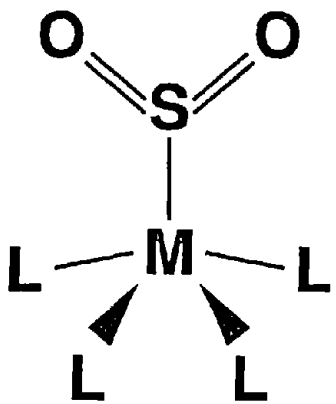

Planar

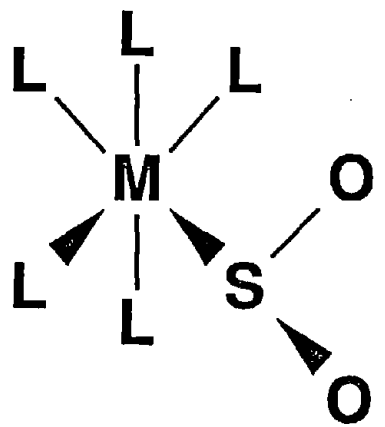

Side-bound

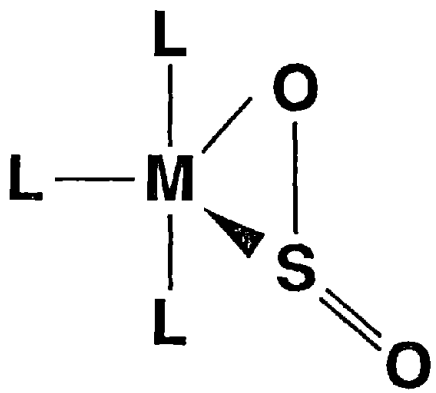

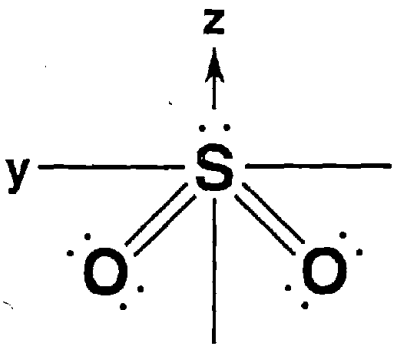
z
y
S
O
O

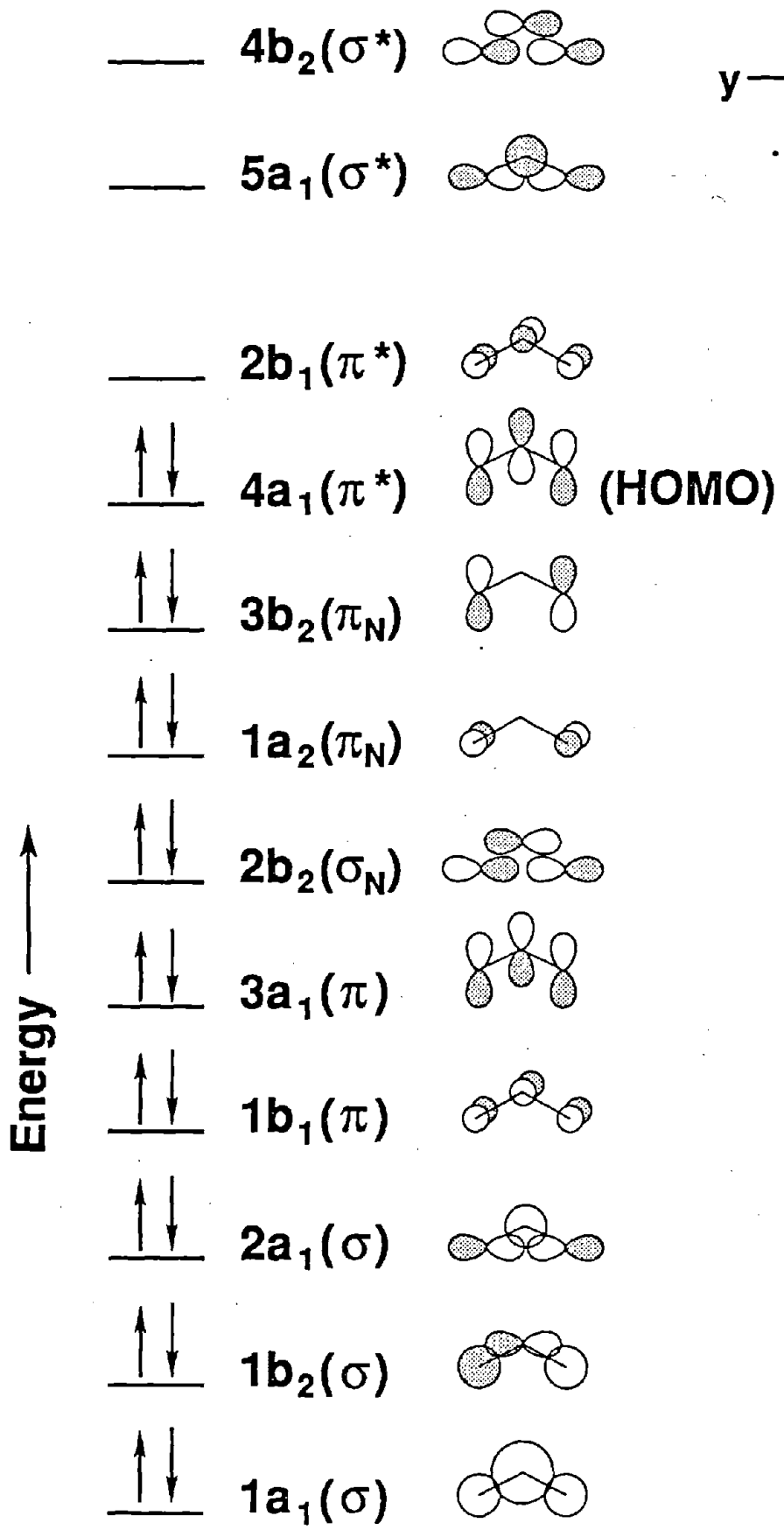
4b2(σ*)
5a1(σ*)
2b1(π*)
4a1(π*)
(HOMO)
3b2(πN)
1a2(πN)
2b2(σN)
3a1(π)
1b1(π)
2a1(σ)
1b2(σ)
1a1(σ)
Energy

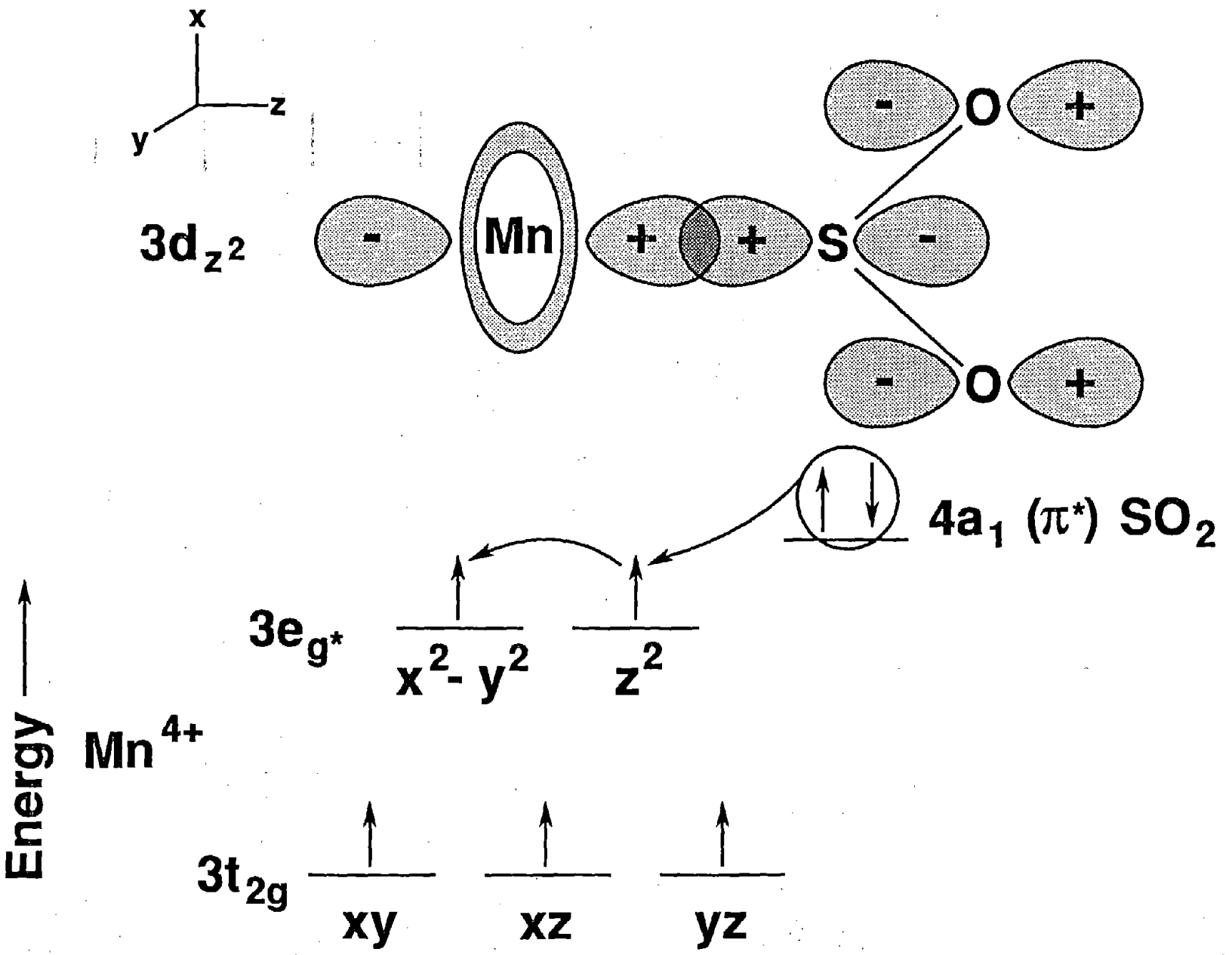
x
z
y
3d$_{z^2}$
-
Mn
+
+
S
O
-
+
O
-
+
4a$_1$ (π^*) SO$_2$
3e$_{g^*}$
x^2- y^2
z^2
Energy
Mn^{4+}
3t$_{2g}$
xy
xz
yz

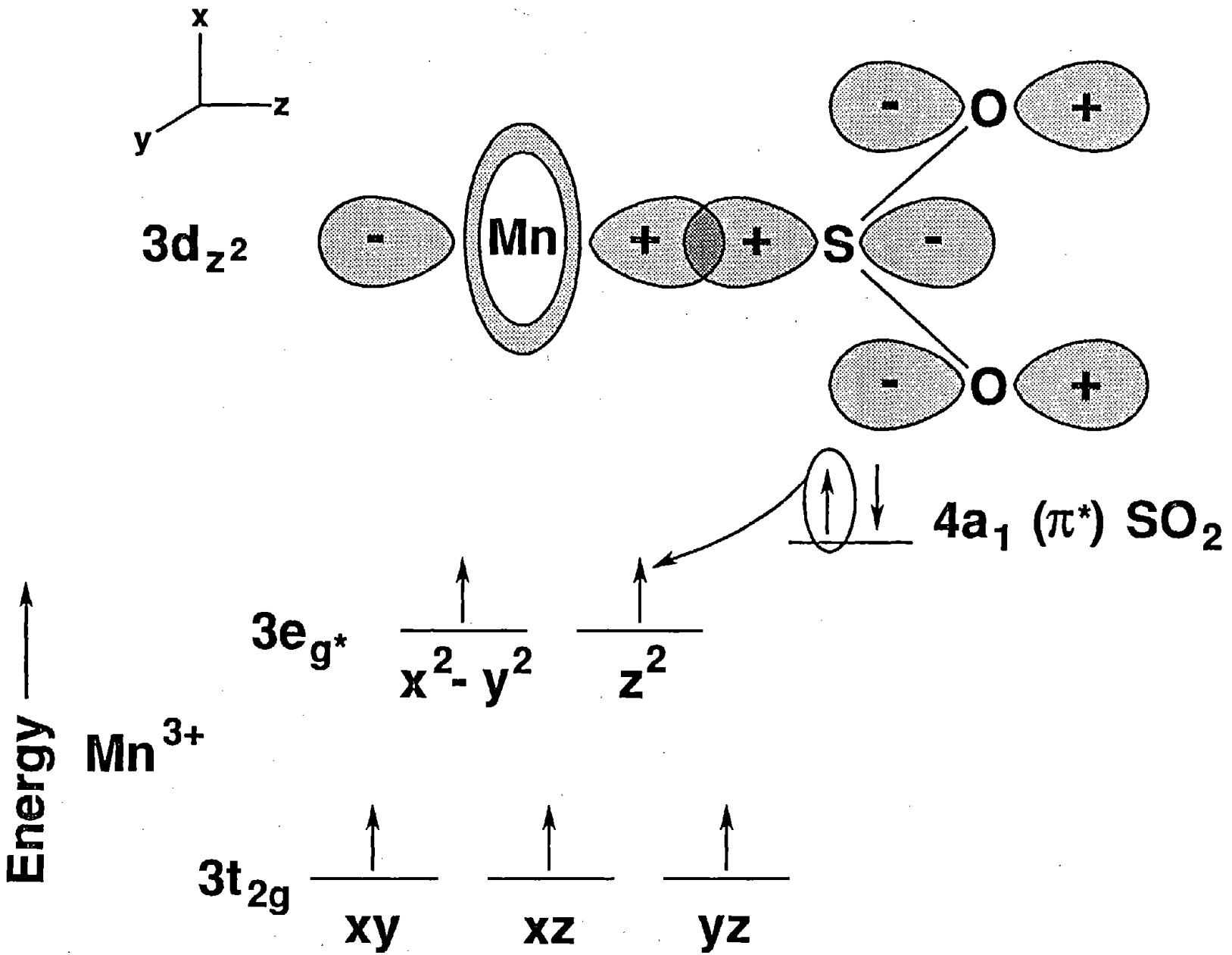
x
z
y
3d$_{z^2}$
Mn
S
O
O
4a$_1$ (π^*) SO$_2$
3e$_{g^*}$
$x^2 - y^2$
z^2
Energy
Mn^{3+}
3t$_{2g}$
xy
xz
yz

Adsorption of reductant

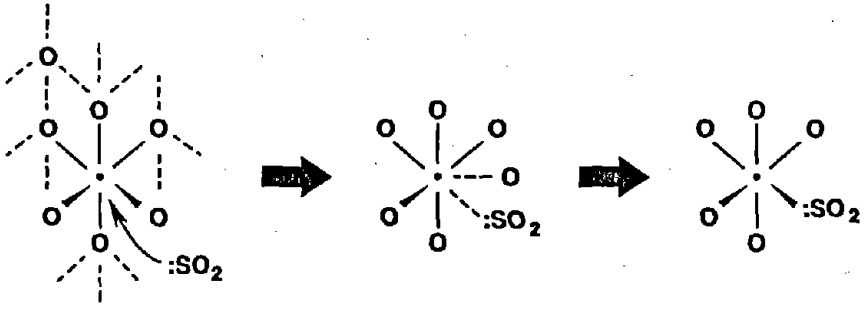

Mn oxides octahedral

Activated complex

Redox precursor

Electron transfer

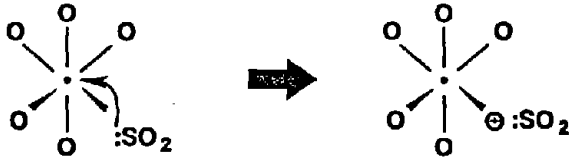

Desorption of $\oplus SO_2$

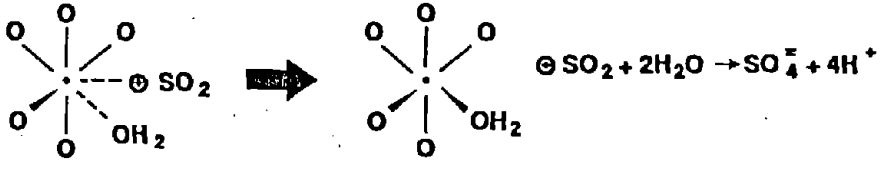

Dissolution of Mn (II) metal center